European Journal of Medicinal Chemistry 224 (2021) 113715

Contents lists available at ScienceDirect

European Journal of Medicinal Chemistry

journal homepage: http://www.elsevier.com/locate/ejmech

Improving the metabolic stability of antifungal compounds based on a scaffold hopping strategy: Design, synthesis, and structure-activity relationship studies of dihydrooxazole derivatives

Liyu Zhao [a], Wenbo Yin [a], Yin Sun [a], Nannan Sun [a], Linfeng Tian [a], Yang Zheng [a], Chu Zhang [a], Shizhen Zhao [b], Xin Su [c], Dongmei Zhao [a, *], Maosheng Cheng [a]

[a] Key Laboratory of Structure-Based Drug Design & Discovery of Ministry of Education, School of Pharmaceutical Engineering, Shenyang Pharmaceutical University, 103 Wenhua Road, Shenhe District, Shenyang, 110016, China
[b] Key Laboratory of Receptor-Mediated Gene Regulation and Drug Discovery, School of Medicine, Henan University, Kaifeng, 475004, China
[c] The School of Life Science and Biopharmaceutical, Shenyang Pharmaceutical University, 103 Wenhua Road, Shenhe District, Shenyang, 110016, China

ARTICLE INFO

Article history:
Received 21 April 2021
Received in revised form
16 July 2021
Accepted 19 July 2021
Available online 21 July 2021

Keywords:
CYP51
Azole antifungals
Metabolic stability
Dihydrooxazole derivatives

ABSTRACT

L-amino alcohol derivatives exhibited high antifungal activity, but the metabolic stability of human liver microsomes *in vitro* was poor, and the half-life of optimal compound **5** was less than 5 min. To improve the metabolic properties of the compounds, the scaffold hopping strategy was adopted and a series of antifungal compounds with a dihydrooxazole scaffold was designed and synthesized. Compounds **A33-A38** substituted with 4-phenyl group on dihydrooxazole ring exhibited excellent antifungal activities against *C. albicans*, *C. tropicalis* and *C. krusei*, with MIC values in the range of 0.03–0.25 μg/mL. In addition, the metabolic stability of compounds **A33** and **A34** in human liver microsomes *in vitro* was improved significantly, with the half-life greater than 145 min and the half-life of 59.1 min, respectively. Moreover, pharmacokinetic studies in SD rats showed that **A33** exhibited favourable pharmacokinetic properties, with a bioavailability of 77.69%, and half-life (intravenous administration) of 9.35 h, indicating that **A33** is worthy of further study.

1. Introduction

In recent decades, the number of HIV/AIDS immunodeficiency patients and patients receiving chemotherapy and organ transplantation has gradually increased, and the rate of invasive fungal infections has been on the rise, posing a serious threat to human health [1–4]. Invasive fungal infections are mainly caused by *Candida*, *Cryptococcus* and *Aspergillus*. Among them, *Candida albicans*, *Cryptococcus neoformans* and *Aspergillus fumigatus* are the three major invasive fungal pathogens [5]. Approximately 72.8 million people suffer from *Candida* spp. infections, 65.5 million people suffer from *Cryptococcus* spp. infections and 12.4 million people suffer from *Aspergillus* spp. infections each year [6]. Although current antifungal treatments are effective, the mortality rate of invasive fungal infections is still very high. Specifically, the mortality rate of invasive *Candida* infection is 20–40 %, that of invasive *Aspergillus* infection is 20–30 % and the fatality rate of other invasive fungal infections is as high as 50 % [7]. The mortality rate of cryptococcal infection varies greatly from 15 % to 70 % in different countries and regions [8,9].

Currently, clinical antifungal agents can be divided into four classes according to the mode of action: polyenes (such as amphotericin B and nystatin) [10], azoles (such as fluconazole and itraconazole) [11], echinocandins (such as caspofungin and micafungin) [12] and antimetabolites (such as 5-fluorocytosine) [13]. Azoles, inhibitors of fungal lanosterol 14α-demethylase (CYP51), can prevent the biosynthesis of ergosterol, which is a very important component of biofilms [14,15]. Due to their high therapeutic index, azole drugs have been used as first-line antifungal agents, and some azole derivatives have been developed, such as fluconazole, itraconazole, voriconazole, and ketoconazole (Fig. 1). However, the narrow antifungal spectrum, serious side effects and the emergence of drug-resistant strains limit the clinical application of azoles [16,17]. Therefore, there is an urgent need to develop antifungal agents with novel structures, low toxicity, and high efficiency.

* Corresponding author.
E-mail address: medchemzhao@163.com (D. Zhao).

https://doi.org/10.1016/j.ejmech.2021.113715
0223-5234/

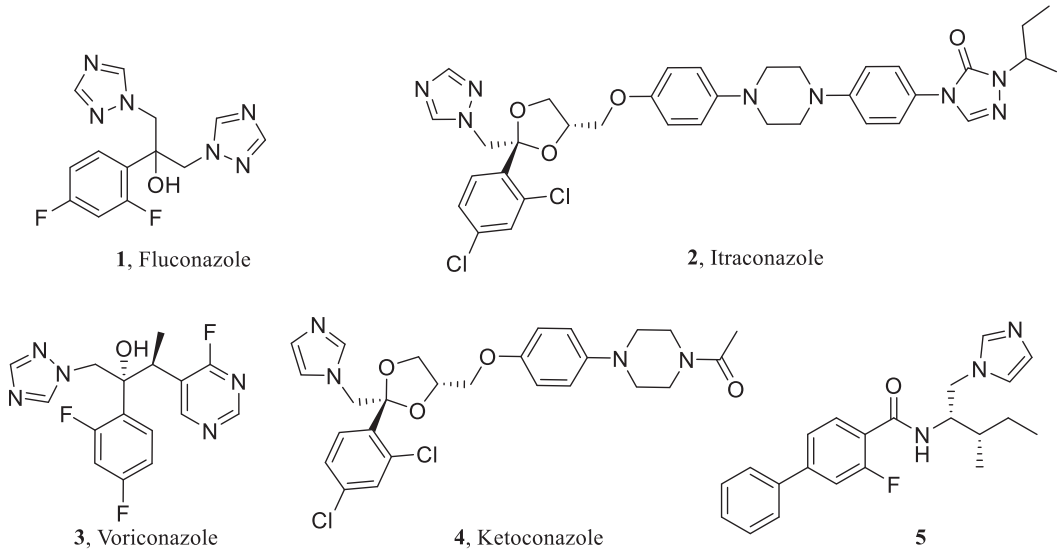

Fig. 1. Chemical structures of azole antifungal agents and lead compound **5**.

Previously, our group reported that a series of L-amino alcohol derivatives exhibited high antifungal activity with a broad spectrum [18]. Unfortunately, the metabolic stability of these compounds is very poor. Optimal compound **5** possessed low metabolic stability in human liver microsomes *in vitro* with a half-life of 3.5 min. Therefore, it is necessary to improve the metabolic properties of these compounds. In this article, through a rational drug design method and a scaffold hopping strategy, a class of novel dihydrooxazole derivatives with stable metabolism *in vitro* and *in vivo* was finally discovered (Fig. 2).

2. Chemistry

Intermediates **8a-m** were prepared conveniently via palladium-catalysed Suzuki coupling of commercially available substituted 4-bromobenzoic acid **6a-c** and substituted phenylboronic **7a-k** (Scheme 1) [19].

Compounds **A1** and **A2** were synthesized as shown in Scheme 2. Intermediate **10** was obtained via an amidation reaction of amino **9** and acid **8a** in DMF at room temperature, which was converted to intermediate **11** through a substitution reaction with imidazole

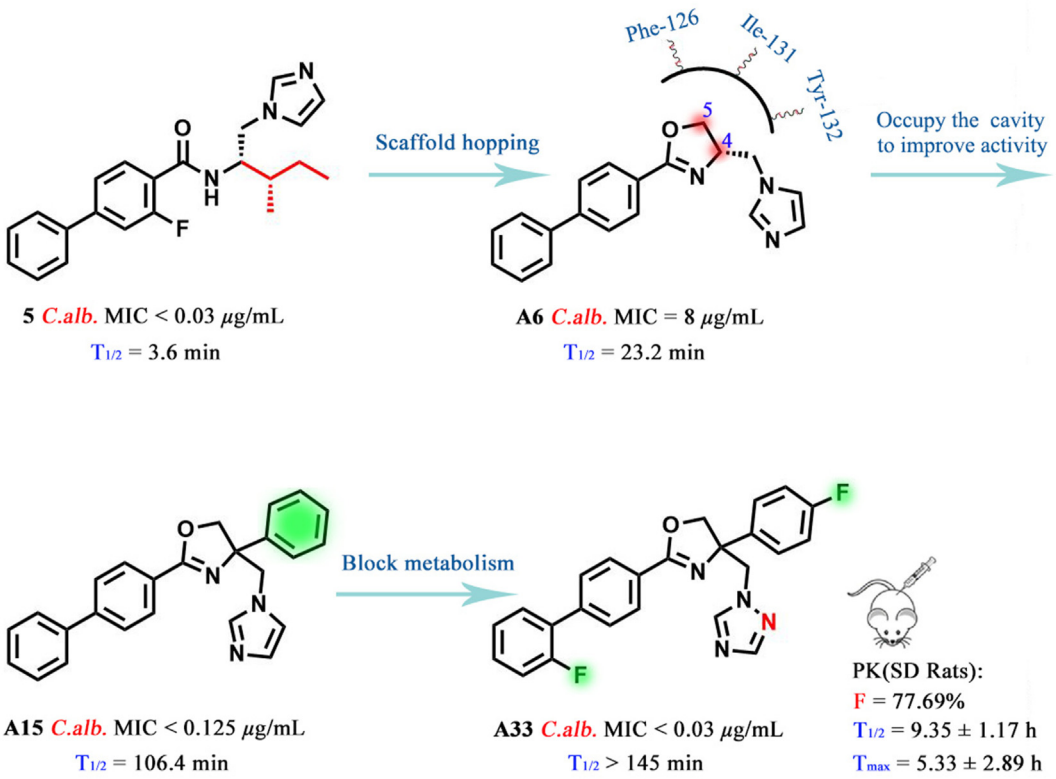

Fig. 2. Design strategies of novel antifungal agents.

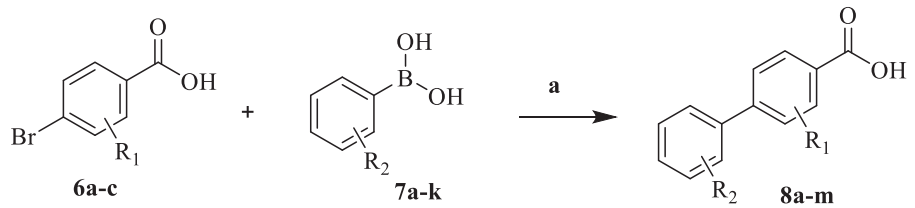

6a	R_2 = H	**7a**	R_2 = H	**7f**	R_2 = 2'-Cl
6b	R_2 = 2-F	**7b**	R_2 = 2'-F	**7g**	R_2 = 3'-Cl
6c	R_2 = 3-F	**7c**	R_2 = 3'-F	**7h**	R_2 = 4'-Cl
		7d	R_2 = 4'-F	**7i**	R_2 = 4'-CN
		7e	R_2 = 3',5'-F,F	**7j**	R_2 = 4'-OCF_3
				7k	R_2 = 4'-CF_3

Scheme 1. The synthetic route of intermediates **8a-m**. Reagents and conditions: (a) $Pd(PPh_3)_4$, K_2CO_3, dioxane/H_2O, reflux, 5 h.

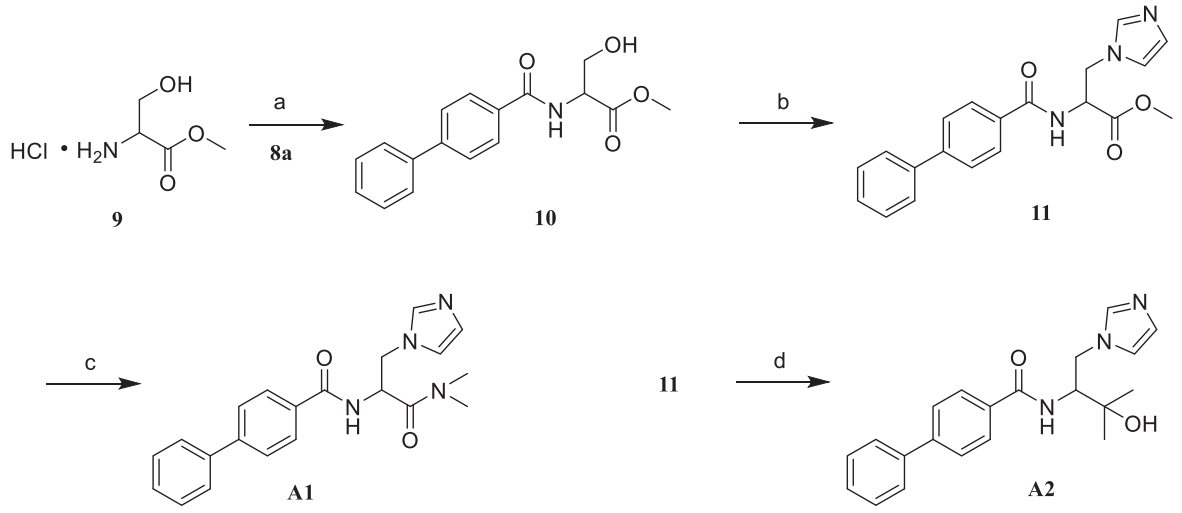

Scheme 2. Synthetic routes of the target compounds **A1** and **A2**. Reagents and conditions: (a) EDCI, HOBt, DIEA, r. t, 4 h; (b) imidazole, CDI, CH_3CN, 70 °C, 5 h; (c) $(CH_3)_2NH$, MeOH, r. t, 5 d; (d) CH_3I, Mg, Et_2O.

[20]. Intermediate **11** was reacted with dimethylamine in alcohol solution to give the target compound **A1**. Intermediate **11** underwent a Grignard reaction to obtain the target compound **A2**.

Compound **A3** was prepared according to the procedures shown in Scheme 3. The Wittig-Horner reaction of **12** with *N*-Cbz-2-phosphoglycine trimethyl ester was carried out to obtain intermediate **13** [21]. The double bond of **13** was reduced to afford intermediate **14**. Protection of the amino group of **14** gave intermediate **15**. Intermediate **16** was obtained by reducing the ester group with $NaBH_4$, which was then converted to **17** through a substitution reaction. Treatment of intermediate **17** with imidazole and NaH in dry DMF afforded intermediate **18**, and then cleavage of the Cbz protecting group with H_2 and Pd/C gave key intermediate **19**. Target compound **A3** was synthesized via an amidation reaction of **19** and **8a** in dry DMF.

As shown in Scheme 4, compounds **A4** and **A5** were synthesized from prolinol by a method similar to that for intermediate **11**.

Compounds **A6-A8** were prepared according to the procedures shown in Scheme 5. Intermediates **23a-c** were obtained via amidation reactions of **22a-b** and **8a**. Then, intermediates **23a-c** were reacted with DAST to afford intermediates **24a-c** [22,23]. Compounds **A6**-**A8** were prepared in a similar manner as that for intermediate **18**, using **24a-c** instead of **15**.

Compound **A9** was synthesized as shown in Scheme 6. Intermediate **27** reacted with $NaNO_2$ in acetic acid solution to obtained **28**, which was reduced under H_2 and Pd/C conditions to give intermediate **29** [24]. The subsequent condensation of **29** with **8a** in the presence of HOBt, EDCI and DIEA produced the corresponding product **30**. Intermediate **31** was obtained by reducing the carbonyl group with $NaBH_4$. Compound **A9** was synthesized from **31**, similar to compounds **A6**-**A8**.

Target compound **A10** was prepared according to the procedures shown in Scheme 7. Intermediate **41** was synthesized using a previously reported method [25,26], which was then reduced with $NaBH_4$ to afford **42**. Intermediate **42** was reacted with DAST to obtain the target compound **A10**.

Compounds **A11** and **A12** were prepared according to the procedures shown in Scheme 8. Under alkaline conditions, intermediate **24a** reacted with CH_3I or BnBr to give intermediates **43a-b**. Compounds **A11** and A**12** were obtained by a method similar to that for compounds **A6-A8**.

Compounds **A13-A14** were synthesized as shown in Scheme 9. Treatment of intermediate **41** with formaldehyde and $NaHCO_3$ in MeOH/H_2O afforded hydroxy derivative **46**, which was then reacted

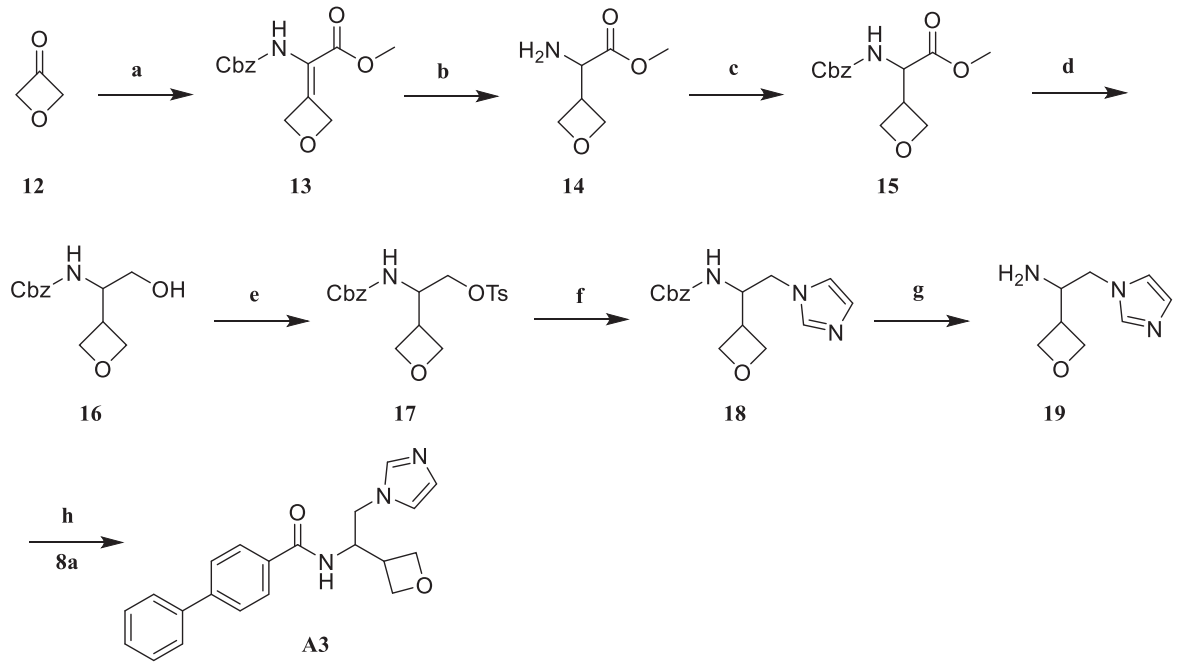

Scheme 3. The synthetic route of target compound **A3**. Reagents and conditions: (a) (±)-Z-α-Phosphonoglycine trimethyl ester, tetramethylguanidine, THF, −70 °C; (b) H_2, $Pd(OH)_2$/C, $MeOH/CH_2Cl_2$, r. t.; (c) Cbz-Cl, TEA, DCM; (d) $NaBH_4$, $MeOH/H_2O$; (e) TsCl, TEA, DMAP, DCM, r. t.; (f) NaH, imidazole, DMF; (g) H_2, Pd/C, MeOH, r. t.; (h) EDCI, HOBt, DIEA, r. t, 4 h.

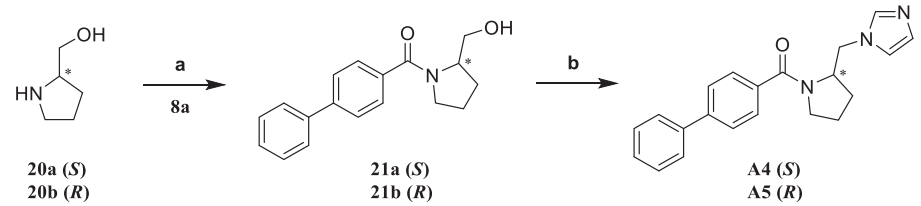

Scheme 4. The synthetic route of target compounds **A4** and **A5**. Reagents and conditions: (a) EDCI, HOBt, DIEA, r. t, 4 h; (b) imidazole, CDI, CH_3CN, 70 °C, 5 h.

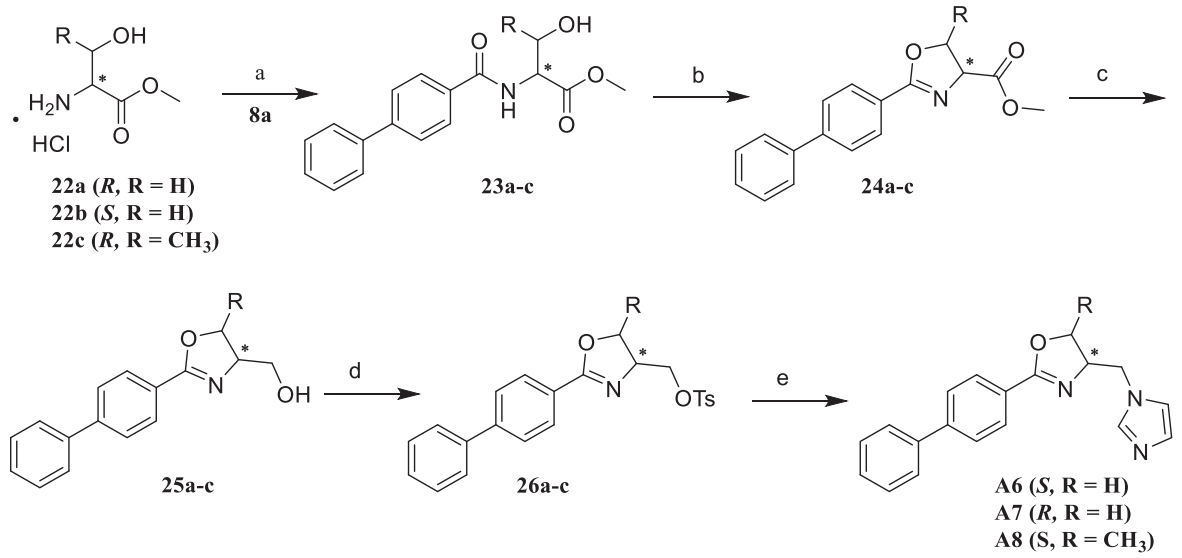

Scheme 5. Synthetic route of target compounds **A6-A8**. Reagents and conditions: (a) EDCI, HOBt, DIEA, r. t, 4 h; (b) DAST, DCM, −78 °C; (c) $NaBH_4$, $MeOH/H_2O$; (d) TsCl, TEA, DMAP, DCM, r. t.; (e) imidazole, NaH, DMF (dry), 80 °C, 12 h.

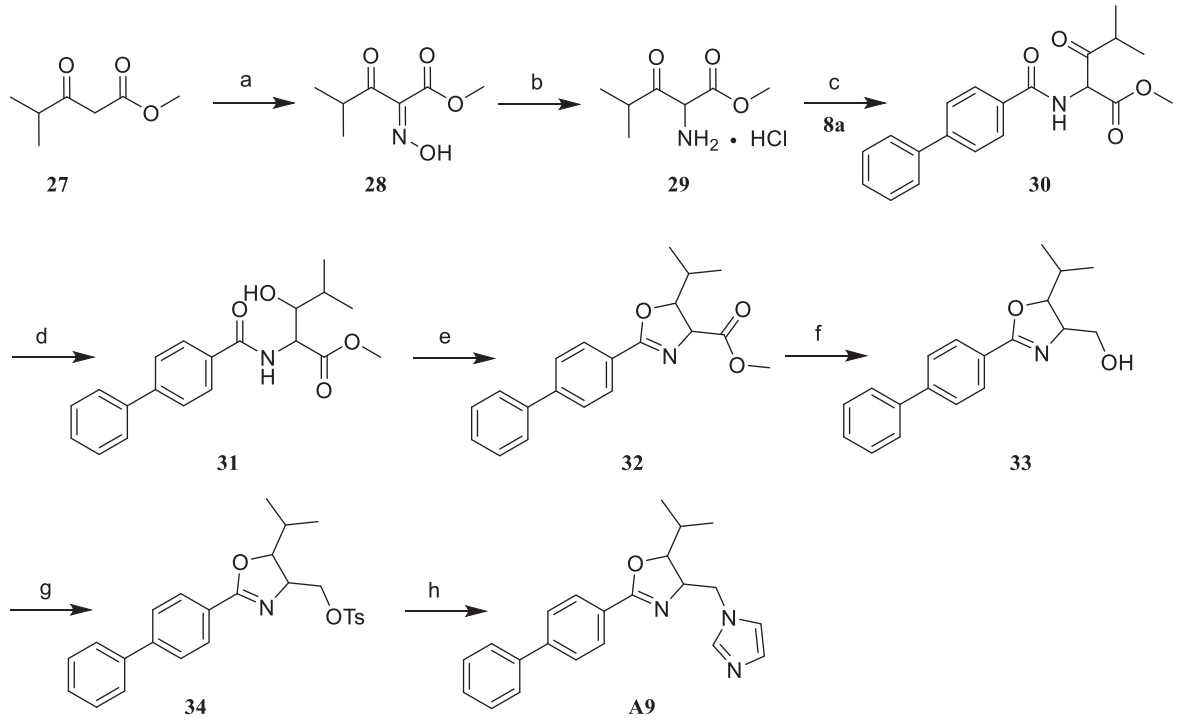

Scheme 6. The synthetic route of target compound **A9**. Reagents and conditions: (a) $NaNO_2$, CH_3COOH, 0 °C; (b) Pd/C, H_2, EtOH/HCl; (c) EDCI, HOBt, DIEA, r. t.; (d) $NaBH_4$, MeOH; (e) $SOCl_2$, MeCN; (f) $NaBH_4$, MeOH/H_2O; (g) TsCl, TEA, DMAP, DCM, r. t.; (h) imidazole, NaH, DMF (dry), 80 °C, 12 h.

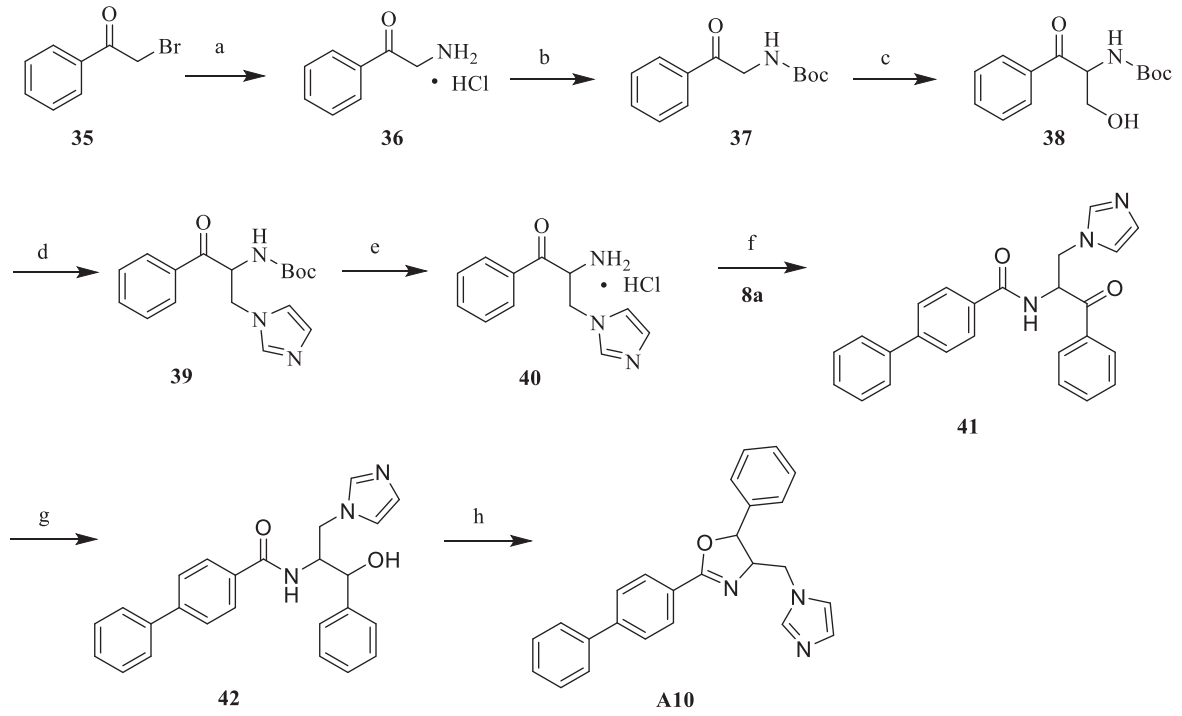

Scheme 7. The synthetic route of target compound **A10**. Reagents and conditions: (a) i) hexamethylenetetramine, $CHCl_3$, 50 °C; ii) 37 % HCl, EtOH, reflux; (b) $(Boc)_2O$, $NaHCO_3$, MeOH, H_2O, r. t.; (c) 37 % CH_2O (aq), $NaHCO_3$, EtOH; (d) imidazole, CDI, CH_3CN, 70 °C; (e) HCl—EtOH, r. t.; (f) HOBt, EDCI, DIEA, DMF, r. t.; (g) $NaBH_4$, MeOH; (h) DAST, DCM.

with DAST at −78 °C to afford compound **A13**. Compound **A13** was reacted with DAST at 30 °C to afford compound **A14**.

The synthesis of dihydrooxazole derivatives **A15**-**A40** was carried out as shown in Scheme 10. Intermediates **48a-f** were obtained by substitution reactions of **47a-f** with $NaNO_2$, which were then reacted with formaldehyde to form intermediates **49a-f**. Dihydroxyl derivatives **49a-f** reacted with 2,2-dimethoxypropane to obtain intermediates **50a-f** [27]. Key intermediates **51a-f** were

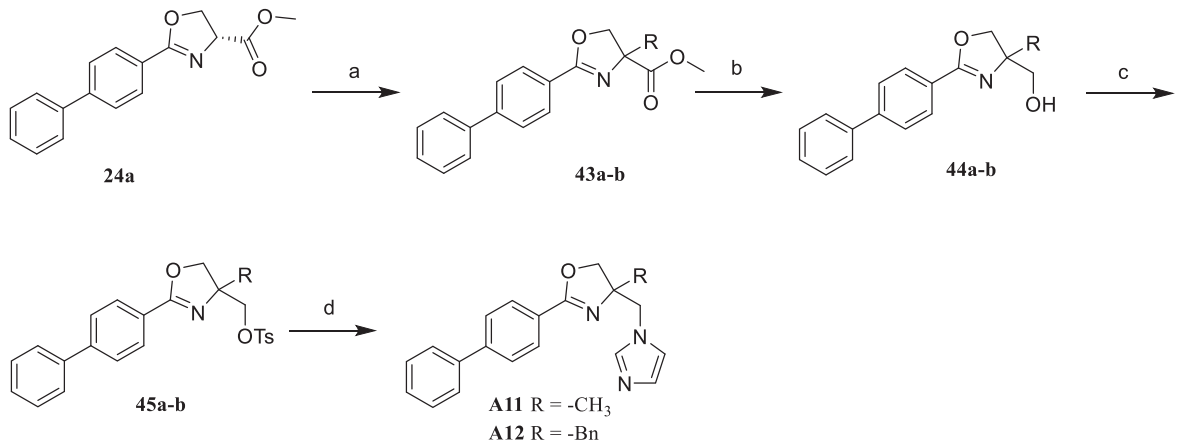

Scheme 8. Synthetic routes of target compounds **A11** and **A12**. Reagents and conditions: (a) LiN(Pr-*i*)$_2$, CH_3I or BnBr, THF, −78 °C; (b) $NaBH_4$, MeOH/H_2O; (c) TsCl, TEA, DMAP, DCM, r. t.; (d) imidazole, NaH, DMF(dry), 80 °C, 12 h.

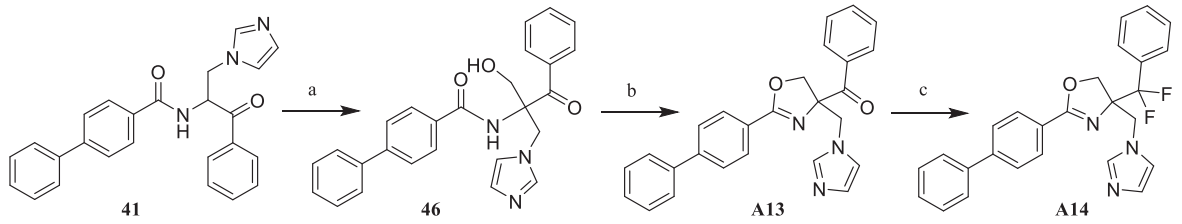

Scheme 9. General synthesis of the target compounds **A13-A14**. Reagents and conditions: (a) 37 % CH_2O (aq), K_2CO_3, EtOH; (b) DAST, DCM, −78 °C; (c) DAST, DCM, 30 °C.

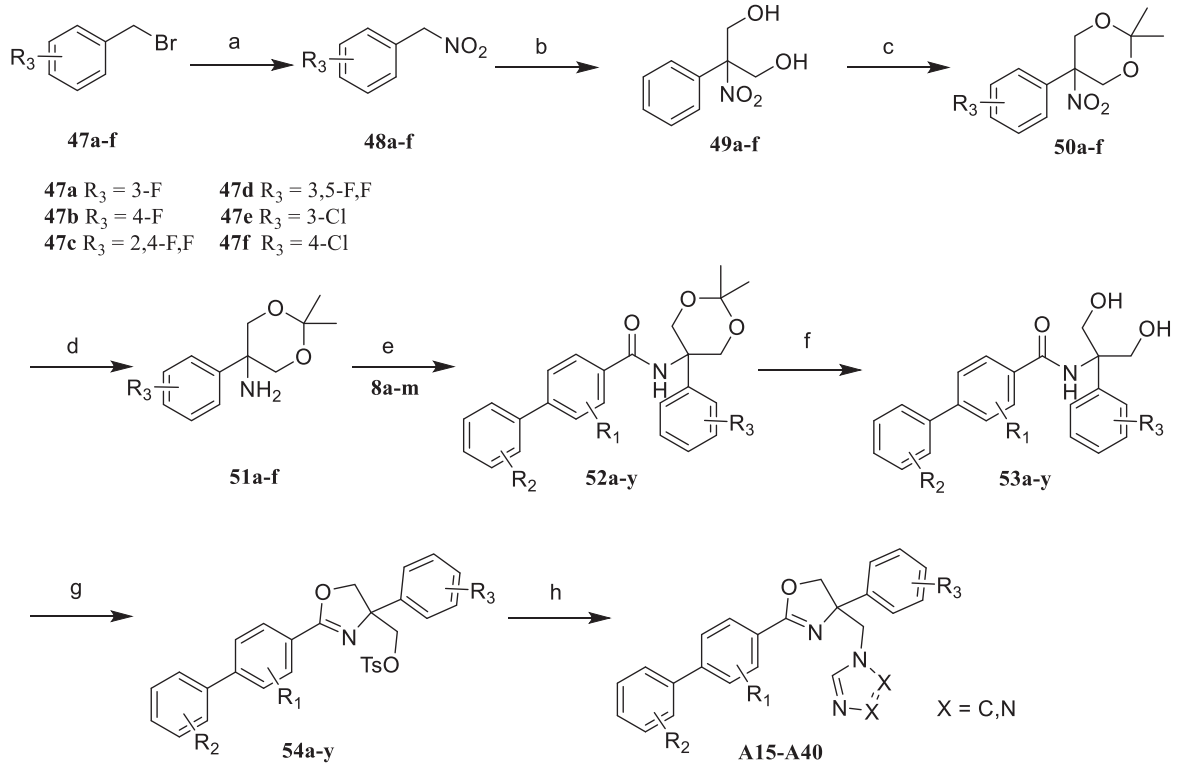

Scheme 10. The synthetic route of target compounds **A15-A40**. Reagents and conditions: (a) $NaNO_2$, NH_2CONH_2, DMF; (b) NaOH, CH_2O(aq), 1,4-diox, EtOH, r. t.; (c) $CH_3C(OCH_3)_2CH_3$, TsOH, acetone; (d) Raney nickel, H_2, EtOH; (e) EDCI, HOBt, DIEA, DMF, 5 h, r. t.; (f) CH_3COOH, H_2O, 60 °C; (g) TsCl, TEA, DMAP, DCM, r. t.; (h) imidazole (or triazole, tetrazole), NaH, DMF (dry), 80 °C, 12 h.

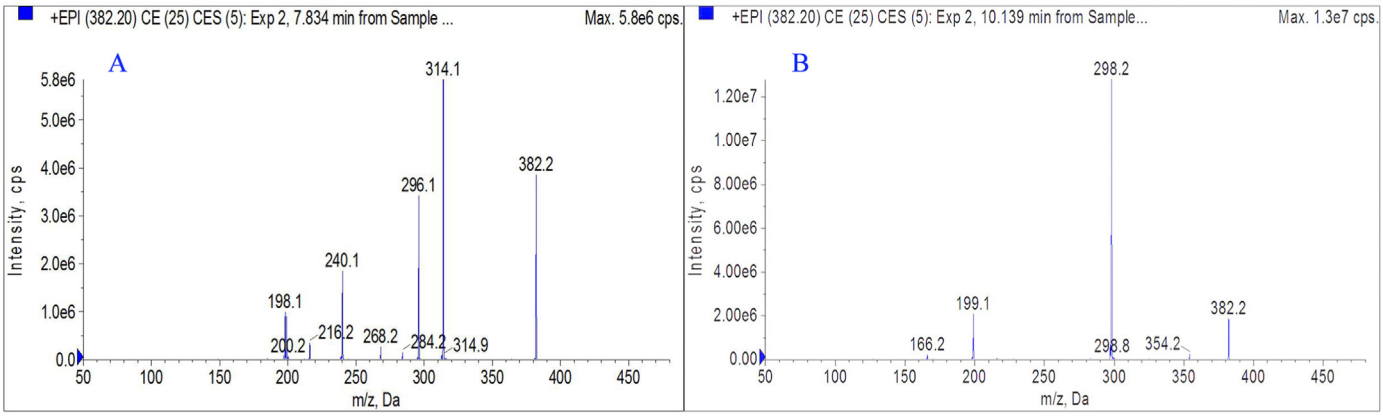

Fig. 3. The fragment ion peaks corresponding to the *in vitro* metabolite $[M+H]^+ = 382$ of compound **5**.

obtained by reducing the nitro group with Raney nickel. Intermediates **52a-y** were synthesized via amidation reactions of amino **51a-f** and acid **8a-m** in DMF, and then cleavage of the ketal protecting group with acetic acid gave intermediates **53a-y**. Compounds **53a-y** were substituted with TsCl and then cyclized to afford intermediates **54a-y**. Treatment of intermediates **54a-y** with imidazole (or triazole, tetrazole) and NaH in dry DMF afforded target compounds **A15**-**A40**.

3. Results and discussion

3.1. Structural modification and in vitro antifungal activity

To improve the metabolic stability of the L-amino alcohol derivatives, compound **5** was selected for an *in vitro* metabolite identification experiment. The first-order ionization results of metabolites showed that the ion peak was 382, and there were two groups of corresponding fragment peaks, namely [314, 296, 240, 216, 198] and [199, 298] (Fig. 3). According to the experimental results, we can infer that the phenyl part of compound **5** may be metabolized by P450 enzymes to form a hydroxyl group (Fig. 3A), and the alkyl part can also be metabolized by P450 enzymes to form a hydroxyl group (Fig. 3B).

Structural modification of the metabolizable alkyl side chain. As shown in Table 1, three strategies were adopted to reduce the oxidative metabolism of the alkyl part and prolong the half-life of the compound. (1) The alkyl side chain was replaced by an amide group, which is not easily metabolized, and compound **A1** was synthesized. (2) The lipophilicity of the compound was reduced, and compounds **A2** and **A3** were synthesized. (3) The scaffold hopping strategy was adopted. Alkyl side chains were eliminated to avoid oxidative metabolism, and compounds **A4-A7** were designed and synthesized. For the oxidative metabolism of the phenyl part, introduction of electron-withdrawing substituents on the benzene ring can block its metabolism.

The *in vitro* antifungal activities were summarized in Table 1. Compared with compound **5**, the antifungal activities *in vitro* of the compounds decreased significantly, or even disappeared completely. Compound **A4** showed weak antifungal activity against *C. alb. (II)* with the MIC value of 32 μg/mL and medium activity against *A. fum.* with the MIC value of 8 μg/mL. Compound **A6** exhibited moderate activity against *C. alb. (II)* (MIC = 8 μg/mL) and *A. fum.* (MIC = 1 μg/mL). Compound **A7**, as the enantiomer of **A6**, did not show antifungal activity, indicating that the chirality of the compound is very important for the antifungal activity. Therefore, **A6** was selected to evaluate the metabolic stability in liver microsomes *in vitro*. The results showed that the stability of compound **A6** was partially improved with a half-life of 23.2 min. Therefore, **A6** was selected for further optimization to discover compounds with good antifungal activity and stable metabolic properties.

Effects of the 4 and 5-position substituents of the dihydrooxazole ring on antifungal activity and metabolic stability. To improve the antifungal activity and metabolic stability of the compound, we studied the binding mode of compound **A6** in the active site of *Candida albicans* CYP51 protein. As shown in Fig. 4, there is a hydrophobic cavity near the 5-position of the dihydrooxazole ring of **A6**. The introduction of a substituent to occupy the hydrophobic cavity may affect the antifungal activity and metabolic stability. Therefore, the small-volume methyl group, the medium-volume isopropyl group and the large-volume phenyl group were introduced to investigate the effect of the 5-position substituent of the dihydrooxazole ring on the antifungal activity and metabolic stability. Compounds **A8-A10** were synthesized, as shown in Table 2.

The introduction of a substituent at the 5-position of the dihydrooxazole ring results in a larger volume and stronger rigidity, which may lead to the compound not being able to enter the active pocket of the CYP51 protein. To improve the flexibility of the compound and occupy the hydrophobic cavity of the CYP51 protein, methyl, benzyl, benzyl derivatives and phenyl groups were introduced at the 4-position of the dihydrooxazole ring. Compounds **A11-A15** were designed and synthesized.

The results of the *in vitro* antifungal activities were summarized in Table 2. Compounds **A8-A10** substituted at the 5th position of the dihydrooxazole ring did not show antifungal activity against *C. alb.* (II) with the MIC values greater than 64 μg/mL.

Compounds **A11**, **A12** and **A15** substituted at the 4th position of the dihydrooxazole ring exhibited increased antifungal activity against *C. alb.* (II) and *C. tro.* The MIC value of methyl-substituted compound **A11** against *C. alb.* (II) was 8 μg/mL and phenyl-substituted compound **A15** against *C. alb.* (II) was 0.125 μg/mL. Moreover, **A11** and **A15** showed moderate antifungal activity against *A. fum.* with MIC values of 0.5 μg/mL and 1 μg/mL, respectively. Since the antifungal activity of **A15** is much higher than that of **A11**, **A15** was selected to evaluate the metabolic stability in human liver microsomes *in vitro*. Fortunately, the results showed that the metabolic stability of compound **A15** was improved significantly, and the half-life was 106.4 min. Next, compound **A15** was selected for further structural optimization.

Structure-activity relationship of the dihydrooxazole derivatives. According to azole groups, azole antifungal drugs can be

Table 1
In vitro antifungal activities of target compounds (MIC, μg/mL)[a]..

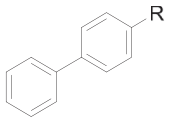

Compd.	R	*C. alb.*(I)	*C. alb.*(II)	*C. neo.*	*A. fum.*
A1	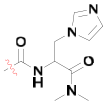	4	>64	>64	>64
A2	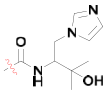	8	>64	>64	>64
A3	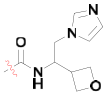	8	>64	>64	>64
A4	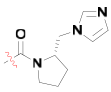	16	32	>64	8
A5	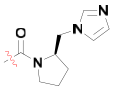	>64	>64	>64	>64
A6	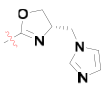	1	8	>64	1
A7	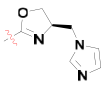	>64	>64	>64	>64
5		<0.03	<0.03	1	2
FCZ		0.5	1	4	>64
ITZ		<0.125	<0.125	<0.125	<0.125

[a]Abbreviations: *C. alb.*(I), *Candida albicans* (SC5314); *C. alb.*(II), *Candida albicans* (CPCC400523); *C. neo.*, *Cryptococcus neoformans* (cgmcc 2.3161); *A. fum.*, *Aspergillus fumigatus* (cgmcc 3.7795); FCZ: fluconazole; ITZ: itraconazole.

divided into imidazoles and triazoles. Clinical studies have shown that the pharmacokinetic properties and side effects of triazole antifungal agents are better than those of imidazole antifungal agents *in vivo*. Therefore, the azole group of dihydrooxazole derivatives was given priority in the investigation. Triazole compound **A16** and tetrazole compound **A17** were synthesized.

The docking results (Fig. 5) showed that the biphenyl group of **A15** occupied the narrow and long hydrophobic cavity of CYP51. Therefore, small volume groups F and Cl were introduced to study the effect on the antifungal activity. The 4′ position of the biphenyl group, towards the entrance of the hydrophobic pocket, is surrounded by amino acid residues that can form hydrogen bond

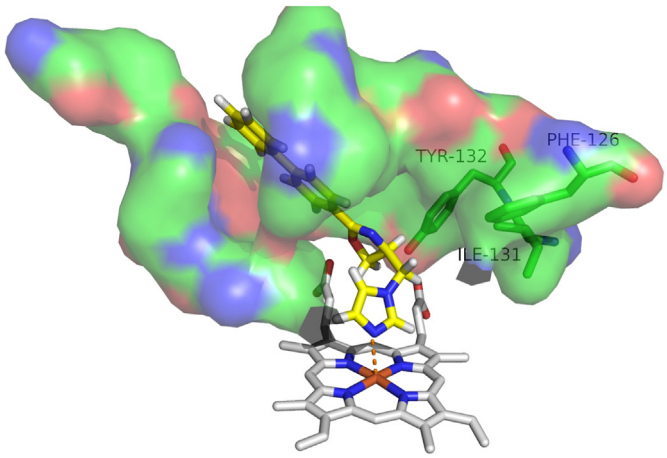

Fig. 4. Predicted binding mode of **A6** in the active site of *Candida albicans* CYP51.

Table 2
In vitro antifungal activities of target compounds (MIC, μg/mL)[a].

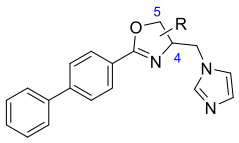

Compd.	R	*C. alb.*(I)	*C. alb.*(II)	*C. tro.*	*C. neo.*	*A. fum.*
A8	5-CH_3	>64	>64	4	>64	>64
A9	5-$CH(CH_3)_2$	0.5	>64	<0.125	>64	>64
A10	5-Ph	>64	>64	>64	>64	>64
A11	4-CH_3	2	8	4	>64	0.5
A12	4-CH_2Ph	<0.125	0.5	0.5	>64	>64
A13	4-COPh	0.5	>64	>64	>64	>64
A14	4-CF_2Ph	<0.125	>64	<0.125	>64	>64
A15	4-Ph	<0.125	<0.125	<0.125	32	1
FCZ	–	0.5	1	1	4	>64
ITZ	–	<0.125	<0.125	<0.125	<0.125	<0.125

[a]Abbreviations: *C. alb.*(I), *Candida albicans* (SC5314); *C. alb.*(II), *Candida albicans* (GIM 2.194); *C. tro.*, *Candida tropicalis* (GIM 2.183); *C. neo.*, *Cryptococcus neoformans* (GIM 2.209); *A. fum.*, *Aspergillus fumigatus* (cgmcc 3.7795); FCZ: fluconazole; ITZ: itraconazole.

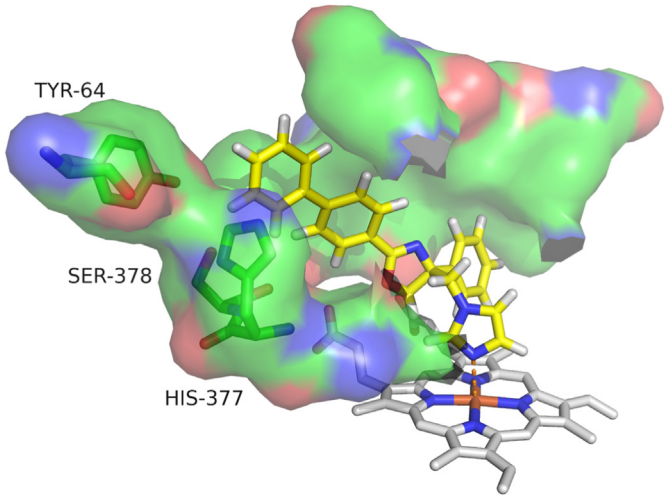

Fig. 5. Predicted binding mode of **A15** in the active site of *Candida albicans* CYP51.

Table 3
In vitro antifungal activities of target compounds (MIC, μg/mL)[a].

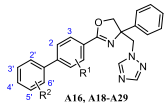

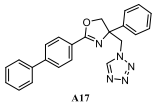

Compd.	R^1	R^2	*C. alb.*(I)	*C. alb.*(II)	*C. tro.*	*C. kru.*	*C. par.*	*A. fum.*
A16	H	H	<0.03	<0.03	0.06	0.25	0.25	2
A17	–	–	>16	>16	>16	>64	>64	>64
A18	2-F	H	<0.03	<0.03	0.06	0.5	4	>64
A19	3-F	H	<0.03	0.06	0.06	>64	16	>64
A20	H	2′-F	<0.03	<0.03	0.06	0.5	16	>64
A21	H	3′-F	<0.03	<0.03	0.06	<0.125	16	>64
A22	H	4′-F	0.25	>16	8	>64	>64	>64
A23	H	3′,5′-F,F	>16	>16	>16	>64	>64	>64
A24	H	2′-Cl	>16	>16	>16	>64	>64	>64
A25	H	3′-Cl	>16	>16	>16	>64	>64	>64
A26	H	4′-Cl	>16	>16	>16	>64	>64	>64
A27	H	4′-CN	>16	>16	>16	>64	>64	>64
A28	H	4′-OCF_3	>16	>16	>16	>64	>64	>64
A29	H	4′-CF_3	>16	>16	>16	>64	>64	>64
FCZ	–	–	0.5	1	1	8	2	>64
ITZ	–	–	<0.03	<0.03	<0.03	<0.125	<0.125	<0.125

[a]Abbreviations: *C. alb.*(I), *Candida albicans* (SC5314); *C. alb.*(II), *Candida albicans* (GIM 2.194); *C. tro.*, *Candida tropicalis* (GIM 2.183); *C. kru.*, *Candida krusei* (GIM 2.1); *C. par.*, *Candida parapsilosis* (GIM 2.190); *A. fum.*, *Aspergillus fumigatus* (cgmcc 3.7795); FCZ: fluconazole; ITZ: itraconazole.

Table 4
In vitro antifungal activities of target compounds (MIC, μg/mL)[a].

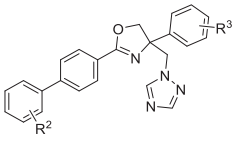

Compd.	R^2	R^3	*C. alb.*(I)	*C. alb.*(II)	*C. tro.*	*C. kru.*	*C. par.*	*A. fum.*
A30	2′-F	3-F	0.06	0.06	0.25	>64	>64	>64
A31	3′-F	3-F	0.06	0.06	0.25	>64	>64	>64
A32	2′-F	3-Cl	0.06	>16	>16	>64	>64	>64
A33	2′-F	4-F	<0.03	<0.03	0.06	0.25	8	>64
A34	3′-F	4-F	<0.03	<0.03	0.06	0.25	8	>64
A35	2′-F	4-Cl	<0.03	<0.03	0.06	0.25	4	>64
A36	3′-F	4-Cl	<0.03	<0.03	0.06	0.25	4	>64
A37	2′-F	2,4-F,F	<0.03	0.06	0.06	0.25	4	>64
A38	3′-F	2,4-F,F	<0.03	0.06	0.06	0.25	>64	>64
A39	2′-F	3,5-F,F	0.06	>16	>16	>64	>64	>64
A40	3′-F	3,5-F,F	0.06	>16	>16	>64	>64	>64
FCZ	–	–	0.5	1	1	8	2	>64
ITZ	–	–	<0.03	<0.03	<0.03	<0.125	<0.125	<0.125

[a]Abbreviations: *C. alb.*(I), *Candida albicans* (SC5314); *C. alb.*(II), *Candida albicans* (GIM 2.194); *C. tro.*, *Candida tropicalis* (GIM 2.183); *C. kru.*, *Candida krusei* (GIM 2.1); *C. par.*, *Candida parapsilosis* (GIM 2.190); *A. fum.*, *Aspergillus fumigatus* (cgmcc 3.7795); FCZ: fluconazole; ITZ: itraconazole.

interactions, e.g. His^{377}, Ser^{378} and Tyr^{64}. Therefore, CN, OCF_3 and CF_3 were also selected for 4′ substitution, with the expectation that the compounds could interact with the surrounding amino acid residues by hydrogen bonds, thereby increasing the antifungal activity and blocking metabolism of the compounds. Compounds **A18-A29** were designed and synthesized.

The results of the *in vitro* antifungal activities were summarized in Table 3. Compared with imidazole compound **A15**, the triazole compound **A16** maintained its antifungal activity against *Candida albicans*, *Candida tropicalis* and *Aspergillus fumigatus*. However, the tetrazole compound **A17** did not show antifungal activity.

Table 5
In vitro antifungal activities of target compounds (MIC, μg/mL)[a].

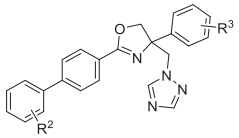

Compd.	R^2	R^3	*Strain CaR*	*Strain 17#*
A30	2′-F	3-F	>64	>64
A31	3′-F	3-F	>64	>64
A33	2′-F	4-F	0.25	>64
A34	3′-F	4-F	0.5	>64
A35	2′-F	4-Cl	0.25	>64
A36	3′-F	4-Cl	0.25	>64
A37	2′-F	2,4-F,F	0.5	>64
A38	3′-F	2,4-F,F	0.5	>64
FCZ	–	–	>64	>64

[a]Abbreviations: *strain CaR*, fluconazole-resistant strain of *Candida albicans*; *strain 17#*, fluconazole and itraconazole resistant strain of *Candida albicans*; FCZ: fluconazole. *Strain 17#* and *strain CaR* were provided by the Institute of Microbiology, Chinese Academy of Sciences.

Therefore, the triazole group was selected as the privileged group for the next structural optimization.

Compounds **A18**-**A21** with F substitution exhibited excellent antifungal activity against *Candida albicans* and *Candida tropicalis*, with MIC values in the range of 0.03−0.06 μg/mL. However, when R^2 was 4′-F or 3′,5′-F,F, the antifungal activity of compounds **A22** and **A23** decreased sharply or even disappeared, with MIC values greater than 16 μg/mL against *Candida albicans* (II). Compounds **A24**-**A29** substituted with 4′-Cl, 4′-CN, 4′-CF_3 or 4′-OCF_3 on the biphenyl group did not show antifungal activity.

Based on the perspective of metabolism, compounds **A18** and **A19** were selected for further structural optimization. Moreover, the predicted binding mode of **A15** in the active site of *Candida albicans* CYP51 showed that the phenyl group on the 4,5-dihydrooxazole ring is close to the ferric porphyrin ring, which is easily metabolized by CYP enzymes. Therefore, the electron-withdrawing substituents F and Cl were selected to block metabolism, and compounds **A30-A40** were designed and synthesized.

The results of the *in vitro* antifungal activities are summarized in Table 4. When R^3 was 4-F, 4-Cl or 2,4-F,F, compounds **A33-A38** exhibited excellent antifungal activity against *Candida albicans* and *Candida tropicalis* with MIC values in the range of 0.03−0.06 μg/mL. Moreover, compounds **A33-A37** exhibited moderate antifungal activity against *Candida krusei* and *Candida parapsilosis* with MIC values in the range of 0.25−8 μg/mL. When R^3 was 3-F, the antifungal activity of compounds **A30** and **A31** was weakened or even disappeared. When R^3 was 3-Cl or 3,5-F,F, the antifungal activity of compounds **A32**, **A39** and **A40** against *Candida albicans* (II) and *Candida tropicalis* decreased significantly, and the MIC values were greater than 16 μg/mL.

3.2. *In vitro* antifungal activity against fluconazole-resistant strains of *Candida albicans*

In recent years, given the widespread use of antifungal agents, fungi have developed severe resistance to marketed drugs, especially fluconazole. Therefore, it is necessary to evaluate the antifungal activity of compounds against fluconazole-resistant strains. The potent compounds **A30**, **A31** and **A33-A38** were selected to evaluate their antifungal activity against fluconazole-resistant strains of *C. albicans* (*strain 17#* and *strain CaR*), which were isolated from AIDS patients. The results were summarized in Table 5.

Table 6
Analysis of sterol composition in *C. albicans* by GC-MS[a].

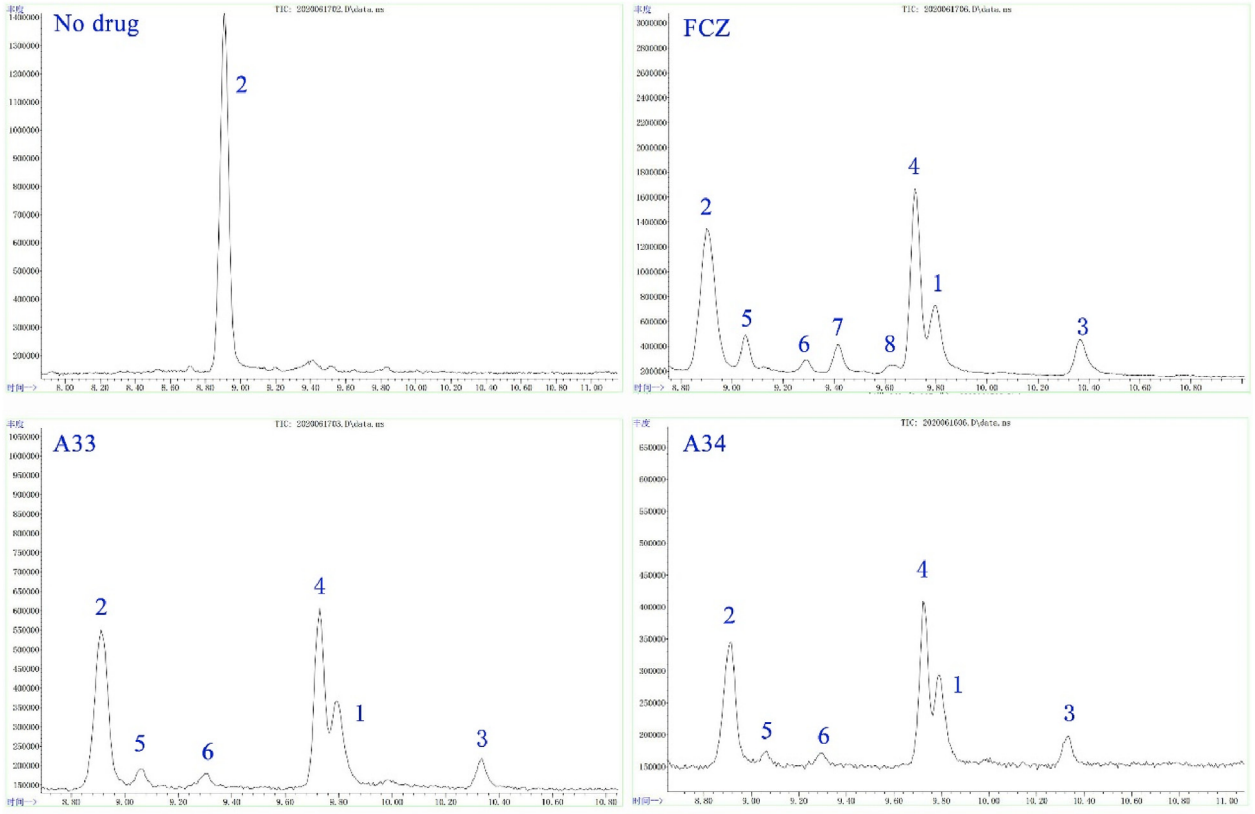

Sterol	% of total sterols (*C. alb.*)			
	No drug	FCZ	A33	A34
Lanosterol (1)	ND	15.13	18.89	18.96
Ergosterol (2)	100.00	34.27	38.82	35.80
Eburicol (3)	ND	7.57	5.08	7.04
14α-methylergosta-8,24 (28)-dien-3β,6α-diol (4)	ND	30.66	32.74	34.14
Unknown sterol (5)	ND	4.31	2.50	1.73
Unknown sterol (6)	ND	1.91	1.97	2.33
Unknown sterol (7)	ND	4.23	ND	ND
Unknown sterol (8)	ND	1.92	ND	ND

[a] Abbreviations: The fungal strain was treated with DMSO (no drug), **FCZ** at 0.25 μg/mL, compounds **A33** and **A34** at 0.015 μg/mL, ND = not detected.

Compounds **A33-A38** showed moderate antifungal activities against *strain CaR* with MIC values in the range of 0.25–0.5 μg/mL. However, the selected compounds did not exhibit inhibitory activity against *strain* 17# with MIC values greater than 64 μg/mL.

3.3. GC-MS analysis of sterol composition in Candida albicans (SC5314)

Dihydrooxazole derivatives are a series of novel antifungal agents. To investigate the antifungal mechanism of compounds **A33** and **A34**, gas chromatography-mass spectrometry (GC-MS) was used to analyse the sterol composition in the cell membrane using fluconazole as the reference drug [28,29]. The sterol profile results were summarized in Table 6. Ergosterol was the only sterol detected in the control group. Compared with the control group, the ergosterol content in the fluconazole group (*Candida albicans* cultured on 1640 medium containing 0.25 μg/mL fluconazole for 18 h) decreased significantly, by 34.27 %. The related sterols, for example lanosterol, eburicol and 14α-methyl ergosta-8,24 (28)-dien-3β,6α-diol, in the ergosterol synthesis pathway accumulated at 15.13 % 7.57 % and 30.66 %, respectively. In addition, some other types of sterols were also detected. These changes in fungal cell membrane sterol composition were caused by inhibiting lanosterol 14α-demethylase (CYP51), a key enzyme in the ergosterol biosynthesis pathway. When *Candida albicans* was treated with compound **A33** at sub-MIC levels of 0.015 μg/mL, the changes in sterol composition were consistent with those of the fluconazole group. The ergosterol content decreased sharply to 38.82 %, and the lanosterol, eburicol and 14α-methyl ergosta-8,24 (28)-dien-3β,6α-diol contents increased to 18.89 %, 5.08 % and 32.74 %, respectively. The change trend of sterol composition of the fungal cell membrane in the compound **A34** group was also similar. The results indicated that **A33** and **A34** exhibited antifungal activity by inhibiting the activity of CYP51 and blocking the biosynthesis of ergosterol.

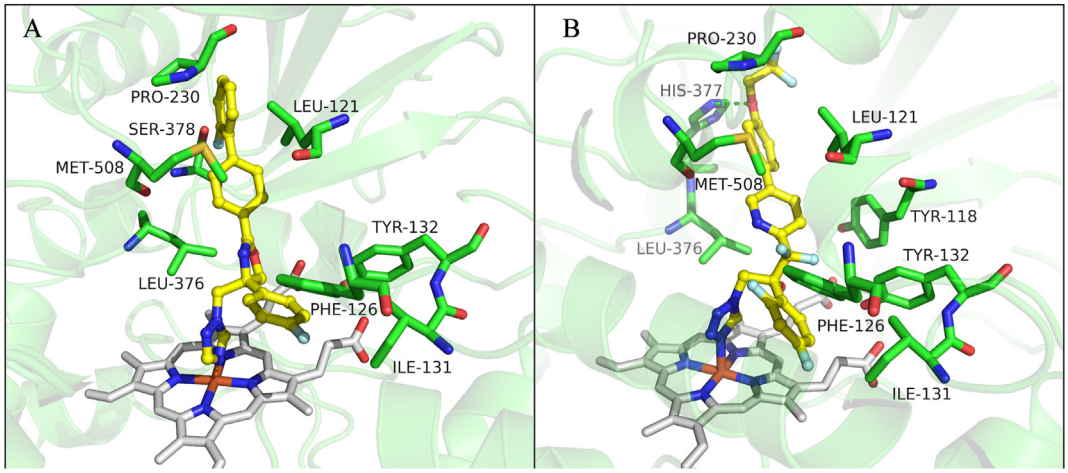

Fig. 6. (A) Predicted binding mode of **A33** in the active site of *Candida albicans* CYP51 (PDB code 5TZ1). (B) Crystal structure of *Candida albicans* CYP51 in complex with **VT-1161** (PDB code 5TZ1). The hydrogen bonds are shown as green dashed lines. Figures were generated using PyMOL.

Table 7
Assessment of metabolic stability in human liver microsomes.

Compd.	HLM 0.5				
	$T_{1/2}$ (min)	$CL_{int(mic)}$ (μL/min/mg)	$CL_{int(liver)}$ (mL/min/kg)	Remaining (T = 60 min)	Remaining (NCF = 60 min)
A33	>145	<9.6	<8.6	75.4 %	89.6 %
A34	59.1	23.5	21.1	47.1 %	79.9 %

NCF: abbreviation of no co-factor. No NADPH regenerating system is added to NCF samples (replaced by buffer) during the 60 min incubation. If the NCF remaining is less than 60 %, then non-NADPH dependent metabolism occurs. $T_{1/2}$: half life. $CL_{int(mic)}$: intrinsic clearance.

Table 8
Assessment of metabolic stability in human plasma.

Compd.	Time Point (min)	% Remaining	$T_{1/2}$ (h)
		Human	Human
A33	60	95.3	>4.8
	120	120.4	
A34	60	98.7	>4.8
	120	115.8	

Table 9
In vitro CYPs inhibition of compounds[a].

Compd.	IC_{50} (μM)				
	CYP1A2	CYP2C9	CYP2C19	CYP2D6	CYP3A4
A33	6.64	2.30	1.56	>50	14.8
A34	21.2	3.80	1.30	40.1	15.2

[a] α-Naphthoflavone (CYP1A2), sulfaphenazole (CYP2C9), ticlopidine (CYP2C19), quinidine (CYP2D6), and ketoconazole (CYP3A4) were used as the positive controls.

3.4. Molecular docking model analysis of compound **A33** in the active site of Candida albicans CYP51

To better understand the binding mode of compounds with *Candida albicans* CYP51, compound **A33** was docked into the active site of *Candida albicans* CYP51. The published crystal structure of *Candida albicans* CYP51 (PDB code 5TZ1) served as a useful template for generating the binding mode [30]. As shown in Fig. 6, the triazole group of the compound **A33** bound to the heme group through the formation of a coordination bond with the iron atom. The 4-fluorophenyl group occupied the hydrophobic cavity and interacted with the surrounding amino acid residues Thr^{126}, Ile^{131} and Tyr^{132}. The biphenyl group extended into the narrow hydrophobic pocket and mainly formed hydrophobic and van der Waals interactions with the surrounding residues, such as Leu^{121}, Pro^{230}, Leu^{376}, Ser^{378} and Met^{508}. The binding mode of **A33** to *Candida albicans* CYP51 was similar to that of compound **VT-1161**.

3.5. Evaluating the metabolic stability of compounds **A33** and **A34**

Metabolic stability is one of the most important challenges in drug discovery. The compound is modified by metabolic enzymes in the body to convert into a larger polar molecule, which accelerates its clearance and reduces its exposure. Therefore, the metabolic stability of compounds is the basis for their exertion and maintenance of their efficacy, and is also an important aspect for evaluating druggability. Drug metabolism mainly occurs in the liver. Therefore, compounds **A33** and **A34** were selected to evaluate the stability in human liver microsomes. The results were summarized in Table 7. Compounds **A33** and **A34** showed favourable metabolic stability in human liver microsomes and compound **A33** substituted with 2′-F was superior to compound **A34** substituted with 3′-F. The half-life of optimal compound **A33** was greater than 145 min.

Enzymes in plasma are different from those in liver microsomes. Human plasma contains a variety of hydrolases, such as cholinesterase, aldolase and lipase. Drug molecules that are not metabolized in the liver may be degraded by hydrolases in plasma. Compounds **A33** and **A34** were selected to evaluate their stability in human plasma. The results were summarized in Table 8. After coincubation with plasma for 120 min, compounds **A33** and **A34** were almost not metabolized by plasma hydrolases, and the half-life values were all greater than 4.8 h, indicating that both compounds possessed good plasma stability.

Table 10
Pharmacokinetic parameters of **A33** after intravenous (iv) and oral (po) administration in SD rats (n = 3) [a].

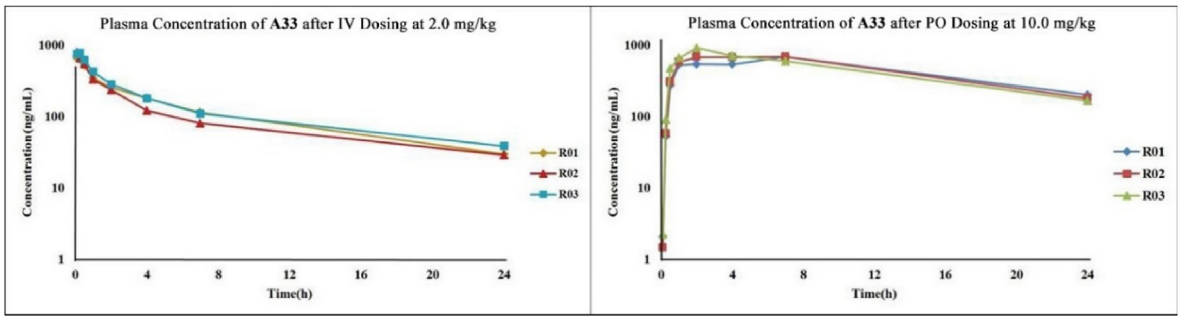

(A) Intravenous Administration (iv)						
Dose (mg/kg)	C_0 (ng/mL)	$T_{1/2}$ (h)	Vd_{ss} (L/kg)	Cl (mL/min/kg)	$AUC_{0\text{-last}}$ (ng·h/mL)	$AUC_{0\text{-inf}}$ (ng.h/mL)
2 mg/kg	758 ± 107	9.35 ± 1.17	7.18 ± 1.10	10.8 ± 1.35	2688 ± 344	3127 ± 398
(B) Oral Administration (po)						
Dose (mg/kg)	C_{max} (ng/mL)	T_{max} (h)	$AUC_{0\text{-last}}$ (ng.h/mL)	$AUC_{0\text{-inf}}$ (ng·h/mL)	F (%)	
10 mg/kg	754 ± 129	5.33 ± 2.89	10,442 ± 181	ND	77.69	

[a] Data are averages of three independent determinations and reported as the mean ± SD (standard deviation). ND = Not determined.

3.6. Cytochrome P450 enzyme inhibition assay

Cytochrome P450 (CYPs) constitute a large class of metal-containing enzymes involved in the metabolism of a wide variety of endogenic and xenobiotic compounds. Among them, drug metabolizing enzymes in humans mainly include CYP1A2, CYP2D6, CYP2C9, CYP2C19 and CYP3A4. It is worth mentioning that CYP3A is involved in 50 % of drug metabolism and CYP2D6 in 30 % of drug metabolism [31]. Because imidazole and triazole groups can coordinate with the Fe^{2+} of the CYP enzymes, azole antifungal drugs generally have a strong inhibitory effect on CYP enzymes. For example, the IC_{50} values of ketoconazole, itraconazole and miconazole against human CYP3A4 were 11.7 nM, 32.6 nM and 74.2 nM, respectively [32]. Compounds **A33** and **A34** were selected to evaluate their inhibitory activities against five major drug-metabolizing enzymes. The results were summarized in Table 9. Compounds **A33** and **A34** showed weak inhibitory effects on CYP3A4 with IC_{50} values greater than 14 μM. In addition, **A33** and **A34** possessed no inhibitory effect on CYP2D6 with IC_{50} values greater than 40 μM. Therefore, **A33** and **A34** are less likely to produce drug-drug interactions.

3.7. Pharmacokinetic assessment in SD rats

On the basis of these favourable *in vitro* profiles, compound **A33** was selected to evaluate its pharmacokinetic properties *in vivo*. As summarized in Table 10, after intravenous administration (iv) at a dose of 2.0 mg/kg, the initial plasma concentration (C_0) of compound **A33** was 758 ± 107 ng/mL, and the half-life ($T_{1/2}$) was 9.35 ± 1.17 h. The area under the curve ($AUC_{0\text{-inf}}$) was 3127 ± 398 ng h/mL. After oral administration (po) at a dose of 10.0 mg/kg, the plasma concentration of compound **A33** was close to the maximum concentration (C_{max}) at 2 h. In addition, **A33** achieved a maximum concentration of 754 ± 129 ng/mL and the $AUC_{0\text{-last}}$ was 10,442 ± 181 ng h/mL. The oral bioavailability (F) of compound **A33** was 77.69 %. According to the experimental results, compound **A33** exhibited favourable pharmacokinetic properties in SD rats.

4. Conclusions

To improve the metabolic stability of L-amino alcohol derivatives, three strategies were adopted, and dihydrooxazole derivative **A6** with moderate antifungal activity was obtained. The metabolic stability of **A6** in liver microsomes was slightly improved and the half-life was 23.2 min. According to the predicted binding mode of **A6** in the active site of *Candida albicans* CYP51, rational drug design was carried out to obtain compound **A15**. The metabolic stability and antifungal activity of **A15** were greatly improved, with a half-life of 106.4 min, and MIC values in the range of 0.03−0.25 μg/mL against *Candida albicans* and *Candida tropicalis*. Then, through a structure-activity relationship study of the dihydrooxazole derivatives, compounds **A30**, **A31** and **A33**-**A38** with excellent antifungal activity were discovered. *In vitro* metabolic stability experiments showed that the optimal compounds **A33** and **A34** possessed excellent metabolic stability in human liver microsomes and plasma. In addition, compounds **A33** and **A34** showed weak or almost no inhibitory effect on CYP3A4 and CYP2D6 and were less likely to produce drug-drug interactions. Pharmacokinetic studies in SD rats showed that **A33** exhibited favourable pharmacokinetic properties and the oral bioavailability was 77.69 %, which is worthy of further research.

5. Experimental section

5.1. Chemistry

All reagents used in the experiment were commercially available without further purification. The solvents were purified according to standard procedures. The reactions were monitored by TLC. TLC was performed on silica gel plates with fluorescence F-254 and visualized with UV light. Silica gel of 200−300 mesh was used for column chromatography. The melting points of the compounds were determined on a BüCHI Melting Point B-540 melting point apparatus and were uncorrected. High-resolution mass spectrometry (HRMS) was performed on an Agilent 6530 accurate-mass Q-TOF LC-MS system. GC−MS analysis was performed on an Agilent 1200 LC−MS using ESI mode. Nuclear magnetic resonance (NMR)

spectra were recorded on a Bruker Avance III-600 or Bruker Avance III-400 instrument (600 or 400 MHz for ^{1}H and 150 or 100 MHz for ^{13}C) with TMS as an internal standard. The coupling constants (*J*) are reported in Hertz, and the peak multiplicities were described as s, singlet; d, doublet; t, triplet; q, quartet; m, multiplet; and br, broad peak.

5.2. General procedure for the synthesis of intermediates ***8a-m***

Under an argon atmosphere, substituted 4-bromobenzoic acid **6a-c** (1.0 equiv.), phenylboronic **7a-k** (1.1 equiv.), K_2CO_3 (2.0 equiv.) and Pd $[P(Ph)_3]_4$ (0.1 equiv) were added to dioxane/H_2O (10:1). The mixture was stirred in a 110 °C oil bath for 5 h. The reaction mixture was cooled to room temperature, and the organic solvent was removed with a vacuum. The residue was dissolved in water, and the solution was acidified with 3 mol/L HCl until the product precipitated. The precipitate was filtered to afford compounds **8a-m**.

5.3. The procedure for the synthesis of intermediate ***10***

To a solution of acid **8a** (2.20 mmol, 0.43 g) in DMF (10 mL), HOBt (2.85 mmol, 0.39 g) and EDCI (2.85 mmol, 0.55 g) were added and the mixture was stirred for 30 min at room temperature. Then, amino salt **9** (2.85 mmol, 0.44 g) and DIEA (5.70 mmol, 0.74 g) were added. The reaction was stirred and monitored with TLC. The mixture was poured into water and extracted with ethyl acetate three times. The combined organic layers were dried over Na_2SO_4 and evaporated under reduced pressure to afford intermediate **10**, yield 76.5 %.

5.4. The procedure for the synthesis of intermediate ***11***

Intermediate **10** (2.0 mmol, 0.6 g), CDI (4.0 mmol, 0.65 g) and imidazole (6.0 mmol, 0.41 g) were added to acetonitrile (20 mL). The mixture was stirred for approximately 5 h at 70 °C and then cooled to room temperature. The organic layer was removed *in vacuo* and the residue was dissolved in ethyl acetate. The organic phase was washed with H_2O three times and then dried over Na_2SO_4 and filtered. The filtrate was concentrated and purified by a silica column to afford intermediate **11**, yield 62.1 %.

5.5. N-(1-(dimethylamino)-3-(1H-imidazole-1-yl)-1-oxopropan-2-yl)-[1,1′-biphenyl]-4-carboxamide (***A1***)

To a solution of dimethylamine in methanol, intermediate **11** was added. The mixture was stirred for approximately 5 d and the organic layer was evaporated *in vacuo*. The residue was purified by silica column to afford **A1**, white solid, yield 43.8 %; mp: 202.3–203.4 °C. ^{1}H NMR (400 MHz, DMSO-d_6)) δ 8.93 (d, J = 8.4 Hz, 1H), 7.93 (d, J = 8.3 Hz, 2H), 7.80–7.71 (m, 4H), 7.64 (s, 1H), 7.50 (t, J = 7.5 Hz, 2H), 7.41 (t, J = 7.3 Hz, 1H), 7.21 (s, 1H), 6.83 (s, 1H), 5.24 (td, J = 8.6, 5.6 Hz, 1H), 4.39 (dd, J = 14.0, 5.4 Hz, 1H), 4.30 (dd, J = 14.0, 8.9 Hz, 1H), 3.05 (s, 3H), 2.86 (s, 3H). ^{13}C NMR (150 MHz, DMSO-d_6) δ 169.45 (s), 166.13 (s), 143.55 (s), 139.57 (s), 138.39 (s), 132.68 (s), 129.51 (s, 2C), 128.61 (s, 4C), 127.37 (s, 2C), 127.00 (s, 2C), 120.53 (s), 50.94 (s), 47.05 (s), 37.07 (s), 35.83 (s). HRMS (ESI, *m/z*) calcd for $C_{21}H_{22}N_4O_2$, $[M+H]^+$, 363.1816; found 363.1850.

5.6. N-(3-hydroxy-1-(1H-imidazole-1-yl)-3-methylbutan-2-yl)-[1,1′-biphenyl]-4-carboxamide (***A2***)

To a solution of ether, magnesium chips (19.20 mmol, 0.46 g) were added, CH_3I (16.06 mmol, 2.28 g) was added dropwise slowly, and the mixture was stirred for 1 h. To a solution of intermediate **11** (4.02 mmol, 1.40 g) in ether at −78 °C, Grignard reagent was added slowly. After dripping, the reaction was raised to room temperature, stirred for 1 h, and then quenched with water. The mixture was extracted with ether three times and the combined organic layers were dried over Na_2SO_4 and evaporated with a vacuum to afford compound **A2**, white solid; yield 70.6 %; mp: 210.3–212.4 °C. ^{1}H NMR (400 MHz, DMSO-d_6) δ 8.17 (d, J = 9.4 Hz, 1H), 7.87 (d, J = 8.4 Hz, 2H), 7.76–7.70 (m, 4H), 7.60 (s, 1H), 7.49 (t, J = 7.5 Hz, 2H), 7.41 (t, J = 7.3 Hz, 1H), 7.13 (s, 1H), 6.79 (s, 1H), 4.82 (s, 1H), 4.43 (dd, J = 13.6, 2.5 Hz, 1H), 4.32–4.24 (m, 1H), 4.15 (dd, J = 13.5, 11.3 Hz, 1H), 1.20 (d, J = 29.2 Hz, 6H). ^{13}C NMR (150 MHz, DMSO-d_6) δ 166.72 (s), 143.23 (s), 139.74 (s), 138.09 (s), 133.74 (s), 129.49 (s, 2C), 128.49 (s), 128.43 (s, 2C), 128.39 (s), 127.37 (s, 2C), 126.93 (s, 2C), 120.24 (s), 71.74 (s), 58.99 (s), 46.02 (s), 28.52 (s), 26.10 (s). HRMS (ESI, *m/z*) calcd for $C_{21}H_{23}N_3O_2$, $[M+H]^+$, 350.1863; found 350.1895.

5.7. The procedure for synthesis of the intermediate ***13***

Under an argon atmosphere, **12** (5.0 mmol, 1.44 g) was added to a mixture of (±)-Z-α-phosphonoglycine trimethyl ester (5.20 mmol, 6.88 g) and tetramethylguanidine (5.0 mmol, 2.52 g) in THF (30 mL) at −70 °C. The reaction mixture was stirred for 1 h and then transferred to room temperature overnight. After filtering, the residue was dissolved in DCM and the organic layer was washed with citric acid (10 %), dried, and concentrated to provide **13** as a white solid, yield 46.5 %.

5.8. The procedure for the synthesis of intermediate ***14***

To a solution of **13** (19.86 mmol, 5.50 g) in DCM (150 mL) and methanol (150 mL), $Pd(OH)_2/C$ (0.43 mmol, 0.30 g) was added. H_2 was bubbled into the reaction mixture at room temperature for 18 h. After filtering, the filtrate was concentrated to provide target compound **14** as yellow oil, yield 81.3 %.

5.9. The procedure for the synthesis of intermediate ***15***

To a solution of **14** (15.85 mmol, 2.30 g) in DCM (50 mL), Cbz-Cl (15.85 mmol, 2.30 mL) and triethylamine (31.71 mmol, 4.40 mL) were added. The mixture was stirred at room temperature for 3 h and then quenched with water (50 mL). The reaction mixture was extracted with DCM. The combined organic extracts were dried, and concentrated under reduced pressure to provide intermediate **15** as oil, yield 76.5 %.

5.10. The procedure for the synthesis of the intermediate ***16***

To a solution of **15** (8.24 mmol, 2.30 g) in methanol (40 mL) and water (10 mL), $NaBH_4$ (41.2 mmol, 1.56 g) was added in portion. After completion of the reaction as indicated by TLC, the reaction mixture was quenched with NH_4Cl (10 mL). The organic layer was removed *in vacuo* and the residue was extracted with ethyl acetate three times. The combined organic extracts were dried and concentrated under reduced pressure to provide title compound **16** as a white solid, yield 65.5 %.

5.11. The procedure for the synthesis of intermediate ***17***

To a mixture of intermediate **16** (2.59 mmol, 0.65 g), TsCl (3.11 mmol, 0.59 g) and DMAP (0.52 mmol, 0.06 g) in DCM (20 mL) was added triethylamine (5.18 mmol, 0.72 mL) at −20 °C. The reaction was stirred overnight and quenched with water. The reaction mixture was washed with citric acid (10 %), and $NaHCO_3$. The organic phase was dried and concentrated to provide a crude product, which was purified by silica gel column chromatography

to afford intermediate **17** as a white solid, yield 82.6 %.

5.12. The procedure for the synthesis of intermediate *18*

Under an argon atmosphere, imidazole (4.94 mmol, 0.34 g) and NaH (9.87 mmol, 0.39 g) were added to dry DMF (20 mL) at 0 °C. The mixture was stirred for 1 h. Then intermediate **18** (2.47 mmol, 1.0 g) was added and stirred at 80 °C for 12 h, controlled by TLC. The reaction was quenched with water and extracted with ethyl acetate three times. The combined organic layers were dried over Na_2SO_4 and evaporated under vacuum. The crude product was purified by silica gel column chromatography (CH_2Cl_2:CH_3OH = 40:1) to provide **18**, yield 50.2 %.

5.13. The procedure for the synthesis of intermediate *19*

To a solution of intermediate **18** (2.46 mmol, 0.74 g) in methanol was added Pd/C (0.25 mmol, 0.26 g, suspended in water), and then H_2 was continuously bubbled in the reaction at room temperature for 18 h. After filtering, the filtrate was concentrated *in vacuo* to afford **19** as colourless oil, yield 78.9 %.

5.14. N-(2-(1H-imidazole-1-yl)-1-(oxetan-3-yl)ethyl)-[1,1′-biphenyl]-4-carboxamide (*A3*)

To a solution of acid **8a** (0.51 mmol, 0.10 g) in DMF (5 mL), HOBt (0.56 mmol, 0.08 g) and EDCI (0.56 mmol, 0.11 g) were added and the mixture was stirred for 1 h at room temperature. Then amino **19** (0.56 mmol, 0.09 g) and DIEA (0.56 mmol, 0.07 g) were added. The reaction was stirred overnight and quenched with water. The reaction mixture was extracted with ethyl acetate three times. The combined organic layers were dried over Na_2SO_4 and evaporated under vacuum. The crude product was purified by silica gel column chromatography (CH_2Cl_2:CH_3OH = 40:1) to afford target compound **A3** as a white solid. Yield 56.3 %; mp: 153.2–155.5 °C. ^{1}H NMR (600 MHz, DMSO-d_6) δ 8.52 (d, J = 8.6 Hz, 1H), 8.03 (s, 1H), 7.89 (d, J = 8.3 Hz, 2H), 7.77 (d, J = 8.3 Hz, 2H), 7.72 (d, J = 7.3 Hz, 2H), 7.50 (t, J = 7.7 Hz, 2H), 7.42 (t, J = 7.3 Hz, 1H), 7.34 (s, 1H), 7.06 (s, 1H), 4.76–4.70 (m, 1H), 4.64 (ddd, J = 18.5, 7.8, 6.3 Hz, 2H), 4.43 (dt, J = 14.3, 6.1 Hz, 2H), 4.19 (dd, J = 14.0, 4.2 Hz, 1H), 4.11 (dd, J = 13.9, 9.1 Hz, 1H), 3.22–3.17 (m, 1H). ^{13}C NMR (150 MHz, DMSO-d_6) δ 166.92 (s), 143.47 (s), 139.63 (s), 137.63 (s), 133.23 (s), 129.51 (s, 2C), 128.57 (s), 128.47 (s, 2C), 127.37 (s, 2C), 126.99 (s, 2C), 126.36 (s), 121.17 (s), 73.50 (s), 73.28 (s), 52.86 (s), 48.05 (s), 37.06 (s). HRMS (ESI, *m/z*) calcd for $C_{21}H_{21}N_3O_2$, $[M+H]^+$, 348.1707; found 348.1740.

5.15. The procedure for the synthesis of compounds *A4* and *A5*

Compounds **A4** and **A5** were prepared in a similar manner as that for intermediate **11**, using **20a-b** instead of **9**.

(S)-(2-((1H-imidazole-1-yl*)methyl)pyrrolidin*-1-yl*) ([1,1′-biphenyl]*-4-yl*)methanone* (**A4**).

White solid, yield 70.4 %; mp: 154.6–156.7 °C. ^{1}H NMR (600 MHz, DMSO-d_6) δ 7.76–7.71 (m, 4H), 7.65–7.59 (m, 3H), 7.49 (t, J = 7.7 Hz, 2H), 7.41 (t, J = 7.4 Hz, 1H), 7.17 (s, 1H), 6.94 (s, 1H), 4.44–4.39 (m, 1H), 4.34 (dd, J = 13.8, 5.7 Hz, 1H), 4.26 (dd, J = 13.8, 3.1 Hz, 1H), 3.36–3.33 (m, 1H), 3.24–3.19 (m, 1H), 1.99–1.94 (m, 1H), 1.70–1.62 (m, 2H), 1.53–1.46 (m, 1H). ^{13}C NMR (150 MHz, DMSO-d_6) δ 168.81 (s), 141.63 (s), 139.28 (s), 137.88 (s), 135.75 (s), 129.04 (s, 2C), 128.49 (s), 127.94 (s), 127.81 (s, 2C), 126.81 (s, 2C), 126.53 (s, 2C), 120.20 (s), 57.09 (s), 49.88 (s), 47.30 (s), 27.41 (s), 24.05 (s). HRMS (ESI, *m/z*) calcd for $C_{21}H_{21}N_3O$, $[M+H]^+$, 332.1757; found 332.1789.

(R)-(2-((1H-imidazole-1-yl*)methyl)pyrrolidin*-1-yl*) ([1,1′-biphenyl]*-4-yl*)methanone* (**A5**).

White solid, mp: 155.6–157.6 °C. ^{1}H NMR (600 MHz, DMSO-d_6) δ 7.76–7.71 (m, 5H), 7.61 (d, J = 8.0 Hz, 2H), 7.50 (t, J = 7.7 Hz, 2H), 7.41 (t, J = 7.3 Hz, 1H), 7.21 (s, 1H), 6.97 (s, 1H), 4.43 (s, 1H), 4.36 (dd, J = 13.8, 5.6 Hz, 1H), 4.27 (dd, J = 13.8, 3.2 Hz, 1H), 3.37–3.33 (m, 1H), 3.26–3.20 (m, 1H), 1.99–1.94 (m, 1H), 1.70–1.62 (m, 2H), 1.54–1.48 (m, 1H). ^{13}C NMR (150 MHz, DMSO-d_6) δ 168.85 (s), 141.63 (s), 139.28 (s), 138.00 (s), 135.71 (s), 129.04 (s, 2C), 128.15 (s), 127.94 (s), 127.81 (s, 2C), 126.80 (s, 2C), 126.51 (s, 2C), 120.44 (s), 57.02 (s), 49.84 (s), 47.50 (s), 27.38 (s), 24.04 (s). HRMS (ESI, *m/z*) calcd for $C_{21}H_{21}N_3O$, $[M+H]^+$, 332.1757; found 332.1788.

5.16. General procedure for the synthesis of intermediates *23a-c*

Intermediates **23a-c** were prepared in a similar manner as that for intermediate **10**, using **22a-c** instead of **9**.

5.17. General procedure for the synthesis of intermediates *24a-c*

Under an argon atmosphere, to a solution of intermediates **23a-c** (1.0 equiv.) in DCM was added DAST (1.2 equiv.) at −78 °C. The reaction was stirred for 1 h and then K_2CO_3 (2.2 equiv.) was added. The reaction mixture was transferred to room temperature, stirred overnight and then quenched with ice water. The reaction mixture was extracted with DCM three times. The organic phase was dried and concentrated to provide a crude product, which was purified by silica gel chromatography to afford intermediates **24a-c** as a white solid.

5.18. General procedure for the synthesis of the compounds *A6-A8*

Compounds **A6-A8** were prepared in a similar manner as that for intermediate **18**, using **24a-c** instead of **15**.

(S)-4-((1H-imidazole-1-yl*)methyl)-2-([1,1′-biphenyl]*-4-yl*)-4,5-dihydrooxazole* (**A6**).

White solid, yield 35.6 %; mp: 134.7–135.6 °C. ^{1}H NMR (600 MHz, DMSO-d_6) δ 7.93 (d, J = 8.4 Hz, 2H), 7.79 (d, J = 8.4 Hz, 2H), 7.74–7.72 (m, 2H), 7.65 (s, 1H), 7.50 (t, J = 7.7 Hz, 2H), 7.42 (t, J = 7.4 Hz, 1H), 7.21 (s, 1H), 6.85 (s, 1H), 4.66–4.61 (m, 1H), 4.51–4.47 (m, 1H), 4.25–4.16 (m, 3H). ^{13}C NMR (150 MHz, DMSO-d_6) δ 163.32 (s), 143.17 (s), 139.03 (s), 137.86 (s), 129.09 (s, 2C), 128.54 (s, 2C), 128.20 (s), 128.18 (s), 126.88 (s, 2C), 126.85 (s, 2C), 120.14 (s), 69.56 (s), 66.44 (s), 49.46 (s). HRMS (ESI, *m/z*) calcd for $C_{19}H_{17}N_3O$, $[M+H]^+$, 304.1444; found 304.1473.

(R)-4-((1H-imidazole-1-yl*)methyl)-2-([1,1′-biphenyl]*-4-yl*)-4,5-dihydrooxazole* (**A7**).

White solid, yield 30.5 %; mp: 145.4–146.3 °C. ^{1}H NMR (600 MHz, DMSO-d_6) δ 7.93 (d, J = 8.1 Hz, 2H), 7.79 (d, J = 8.1 Hz, 2H), 7.73 (d, J = 7.8 Hz, 2H), 7.70 (s, 1H), 7.50 (t, J = 7.6 Hz, 2H), 7.42 (t, J = 7.2 Hz, 1H), 7.23 (s, 1H), 6.88 (s, 1H), 4.67–4.62 (m, 1H), 4.49 (t, J = 9.2 Hz, 1H), 4.27–4.17 (m, 3H). ^{13}C NMR (150 MHz, DMSO-d_6) δ 163.34 (s), 143.18 (s), 139.03 (s), 137.84 (s), 129.10 (s, 2C), 128.55 (s, 2C), 128.21 (s), 128.04 (s), 126.88 (s, 2C), 126.86 (s, 2C), 126.03 (s), 120.21 (s), 69.56 (s), 66.42 (s), 49.52 (s). HRMS (ESI, *m/z*) calcd for $C_{19}H_{17}N_3O$, $[M+H]^+$, 304.1444; found 304.1473.

(4S,5R)-4-((1H-imidazole-1-yl*)methyl)-2-([1,1′-biphenyl]*-4-yl*)-5-methyl-4,5-dihydrooxazole* (**A8**).

White solid, yield 30.6 %; mp: 110.1–112.8 °C. ^{1}H NMR (600 MHz, DMSO-d_6) δ 7.92 (d, J = 8.4 Hz, 2H), 7.78 (d, J = 8.5 Hz, 2H), 7.74–7.72 (m, 2H), 7.67 (s, 1H), 7.50 (t, J = 7.7 Hz, 2H), 7.42 (t, J = 7.4 Hz, 1H), 7.24 (s, 1H), 6.87 (s, 1H), 4.59–4.55 (m, 1H), 4.28–4.21 (m, 2H), 4.15–4.11 (m, 1H), 1.27 (d, J = 6.3 Hz, 3H). ^{13}C NMR (150 MHz, DMSO-d_6) δ 163.01 (s), 143.59 (s), 139.51 (s), 138.23 (s), 129.55 (s, 2C), 128.97 (s, 2C), 128.62 (d, J = 10.8 Hz), 127.30 (s, 4C), 126.74 (s), 120.53 (s), 78.95 (s), 73.45 (s), 49.74 (s), 20.90 (s). HRMS (ESI, *m/z*) calcd for $C_{20}H_{19}N_3O$, $[M+H]^+$, 318.1601; found 318.1630.

5.19. The procedure for the synthesis of intermediate **28**

To a solution of methyl **27** (20.81 mmol, 3.0 g) in glacial acetic acid, $NaNO_2$ (52.02 mmol, 3.59 g) was added. The reaction mixture was stirred at 0 °C for 2 h, and then transferred to room temperature for another 3 h. After completion of the reaction as indicated by TLC, the reaction mixture was poured into water and extracted with ether three times. The combined extracts were washed with aqueous $NaHCO_3$ and NaCl and then dried and concentrated under reduced pressure to provide **28** as light-yellow oil, yield 70.3 %.

5.20. The procedure for the synthesis of intermediate **29**

To a solution of **28** in ethanol was added Pd/C (0.1 equiv.). H_2 was bubbled into the reaction at room temperature for 1 h. Then HCl/EtOH (8.0 equiv.) was added to the reaction. After filtering, the filtrate was concentrated to provide **29** as a white solid, yield 82.3 %.

5.21. The procedure for the synthesis of intermediate **30**

Intermediate **30** was prepared in a similar manner as that for intermediate **10**, using **29** instead of **9**. White solid, yield 50.7 %.

5.22. The procedure for the synthesis of intermediate **31**

To a solution of **30** (1.47 mmol, 0.50 g) in methanol (15 mL), $NaBH_4$ (0.37 mmol, 0.01 g) was added in portion. After completion of the reaction as indicated by TLC, the reaction mixture was quenched with aqueous NH_4Cl (3 mL). After filtering, the solvent was removed with a vacuum and the residue was purified by silica gel chromatography to provide intermediate **31** as a white solid, yield 56.2 %.

5.23. The procedure for the synthesis of the compound **A9**

Compound **A9** was prepared in a similar manner as that for compounds **A6-A8**, using **31** instead of **23a-c**. White solid, yield 49.8 %; mp: 88.5–91.7 °C. ^{1}H NMR (600 MHz, DMSO-d_6) δ 7.94 (d, J = 8.5 Hz, 2H), 7.79 (d, J = 8.5 Hz, 2H), 7.75–7.69 (m, 3H), 7.50 (t, J = 7.7 Hz, 2H), 7.42 (t, J = 7.4 Hz, 1H), 7.27 (s, 1H), 6.87 (s, 1H), 4.29–4.15 (m, 4H), 1.75 (dt, J = 13.3, 6.6 Hz, 1H), 0.82 (dd, J = 19.1, 6.7 Hz, 6H). ^{13}C NMR (150 MHz, DMSO-d_6) δ 163.28 (s), 143.66 (s), 139.56 (s), 138.34 (s), 129.55 (s, 2C), 128.95 (s, 2C), 128.70 (s), 128.65 (s), 127.38 (s, 2C), 127.33 (s, 2C), 126.60 (s), 120.64 (s), 86.75 (s), 69.28 (s), 50.43 (s), 32.05 (s), 17.24 (s), 17.04 (s). HRMS (ESI, m/z) calcd for $C_{22}H_{23}N_3O$, $[M+H]^+$, 346.1914; found 346.1945.

Intermediate **41** was synthesized according to a previous report [26].

5.24. The procedure for the synthesis of intermediate **42**

Intermediate **42** was prepared in a similar manner as that for intermediate **31**, using **41** instead of **30**. White solid, yield 65.2 %.

5.25. The procedure for the synthesis of compound **A10**

Compound A**10** was prepared in a similar manner as that for intermediates **24a-c**, using **42** instead of **23a-c**. White solid, yield 61.6 %; mp: 140.0–142.6 °C. ^{1}H NMR (400 MHz, DMSO-d_6) δ 8.02 (d, J = 8.5 Hz, 2H), 7.82 (d, J = 8.5 Hz, 2H), 7.79 (s, 1H), 7.77–7.72 (m, 2H), 7.51 (t, J = 7.5 Hz, 2H), 7.43 (t, J = 7.3 Hz, 1H), 7.40–7.29 (m, 4H), 7.19–7.13 (m, 2H), 6.89 (s, 1H), 5.51 (d, J = 6.0 Hz, 1H), 4.47–4.31 (m, 3H). ^{13}C NMR (100 MHz, DMSO-d_6) δ 163.33 (s), 143.94 (s), 140.87 (s), 139.52 (s), 138.41 (s), 129.57 (s, 2C), 129.27 (s, 2C), 129.20 (s), 128.85 (s), 128.73 (s, 2C), 127.48 (s, 2C), 127.36 (s, 2C), 126.25 (s), 125.63 (s), 120.66 (s), 82.98 (s), 75.60 (s), 50.00 (s). HRMS (ESI, m/z) calcd for $C_{25}H_{21}N_3O$, $[M+H]^+$, 380.1757; found 380.1792.

5.26. General procedure for the synthesis of intermediates **43a-b**

Under an argon atmosphere, to a solution of intermediate **24a** (1.0 equiv.) in anhydrous THF, LiN(Pr-i)$_2$ (1.5 equiv.) was added dropwise at −78 °C. The reaction mixture was stirred for 1 h and CH_3I or BnBr was added (2.5 equiv.). Stirring was continued for another 1 h. The resulting mixture was allowed to warm to room temperature and quenched with saturated aqueous NH_4Cl solution. The product was extracted with ethyl acetate, followed by drying over Na_2SO_4 and removal of the solvent under reduced pressure. Purification by flash column chromatography yielded a white solid of title intermediates **43a-b**.

5.27. The procedure for the synthesis of compounds **A11-A12**

Compounds **A11-A12** were prepared in a similar manner as that for intermediate **18**, using **43a-b** instead of **15**.

4-((1H-imidazole-1-yl*)methyl)-2-([1,1′-biphenyl]*-4-yl*)-4-methyl-4,5-dihydrooxazole* (**A11**).

White solid, yield 49.7 %. ^{1}H NMR (400 MHz, DMSO-d_6) δ 7.90 (d, J = 8.4 Hz, 2H), 7.77 (d, J = 8.4 Hz, 2H), 7.74–7.70 (m, 2H), 7.59 (s, 1H), 7.50 (t, J = 7.5 Hz, 2H), 7.41 (t, J = 7.3 Hz, 1H), 7.14 (s, 1H), 6.81 (s, 1H), 4.31 (d, J = 8.9 Hz, 1H), 4.22–4.14 (m, 2H), 4.12 (d, J = 8.9 Hz, 1H), 1.31 (s, 3H). ^{13}C NMR (150 MHz, DMSO-d_6) δ 162.53 (s), 143.58 (s), 139.51 (s), 138.65 (s), 129.56 (s, 2C), 129.00 (s, 2C), 128.65 (s), 128.29 (s), 127.30 (s, 2C), 126.54 (s), 121.09 (s), 75.01 (s), 71.27 (s), 54.27 (s), 25.11 (s). HRMS (ESI, m/z) calcd for $C_{20}H_{19}N_3O$, $[M+H]^+$, 318.1601; found 318.1632.

4-((1H-imidazole-1-yl*)methyl)-2-([1,1′-biphenyl]*-4-yl*)-4-benzyl-4,5-dihydrooxazole* (**A12**).

White solid, yield 52.3 %; mp: 136.0–137.8 °C. ^{1}H NMR (400 MHz, DMSO-d_6) δ 7.81 (d, J = 8.5 Hz, 2H), 7.75–7.68 (m, 4H), 7.61 (s, 1H), 7.49 (t, J = 7.5 Hz, 2H), 7.41 (t, J = 7.3 Hz, 1H), 7.28–7.14 (m, 6H), 6.81 (s, 1H), 4.31 (s, 2H), 4.23 (d, J = 9.2 Hz, 1H), 4.16 (d, J = 9.2 Hz, 1H), 3.04 (d, J = 13.5 Hz, 1H), 2.91 (d, J = 13.5 Hz, 1H). ^{13}C NMR (150 MHz, DMSO-d_6) δ 162.96 (s), 143.59 (s), 139.55 (s), 138.77 (s), 136.51 (s), 131.09 (s, 2C), 129.54 (s, 3C), 128.89 (s, 2C), 128.63 (s), 128.44 (s, 2C), 127.31 (s, 4C), 127.01 (s), 126.39 (s), 121.17 (s), 74.67 (s), 71.66 (s), 53.85 (s), 42.88 (s). HRMS (ESI, m/z) calcd for $C_{26}H_{23}N_3O$, $[M+H]^+$, 394.1914; found 394.1949.

5.28. The procedure for the synthesis of intermediate **46**

To a solution of intermediate **41** (2.0 mmol, 0.79 g) in ethanol, K_2CO_3 (1.0 mmol, 0.14 g) and 37 % CH_2O (60.0 mmol, 0.79 g) were added. The mixture was stirred at 35 °C for 5 h, and then the organic solvent was removed with a vacuum. The residue was dissolved in DCM and washed with water and brine sequentially. The organic phase was dried over Na_2SO_4 and filtered. The filtrate was concentrated and purified by silica column to give intermediate **46** as a white solid, yield 40.0 %.

5.29. The procedure for the synthesis of compound **A13**

Compound **A13** was prepared in a similar manner as that for intermediates **24a-c**, using **46** instead of **23a-c**. White solid, yield 51.3 %. ^{1}H NMR (400 MHz, DMSO-d_6) δ 8.31–8.26 (m, 2H), 7.96 (d, J = 8.5 Hz, 2H), 7.80 (d, J = 8.5 Hz, 2H), 7.75–7.71 (m, 2H), 7.67 (t, J = 7.4 Hz, 1H), 7.60 (s, 1H), 7.56 (t, J = 7.6 Hz, 2H), 7.50 (t, J = 7.5 Hz, 2H), 7.42 (t, J = 7.3 Hz, 1H), 7.13 (s, 1H), 6.79 (s, 1H), 4.95 (d, J = 9.6 Hz, 1H), 4.71 (d, J = 14.3 Hz, 1H), 4.60 (d, J = 9.7 Hz, 1H), 4.55 (d, J = 14.3 Hz, 1H). ^{13}C NMR (150 MHz, DMSO-d_6) δ 199.02 (s),

164.80 (s), 144.24 (s), 139.41 (s), 138.85 (s), 135.43 (s), 134.00 (s), 130.51 (s, 2C), 129.57 (s, 2C), 129.27 (s, 2C), 129.01 (s, 2C), 128.78 (s), 128.54 (s), 127.48 (s, 2C), 127.38 (s, 2C), 125.80 (s), 121.16 (s), 83.65 (s), 72.39 (s), 52.55 (s). HRMS (ESI, *m/z*) calcd for $C_{26}H_{21}N_3O_2$, $[M+H]^+$, 408.1707; found 408.1743.

5.30. The procedure for the synthesis of compound ***A14***

Under an argon atmosphere, DAST (1.15 mmol, 0.19 g) was added to a solution of compound **A13** (1.0 mmol, 0.41 g) in DCM at 0 °C. The reaction was stirred for 1 h at 30 °C, and then K_2CO_3 was added (2.0 mmol, 0.28 g). The reaction mixture was stirred overnight and then quenched with ice water. The reaction mixture was extracted with DCM three times. The organic phase was dried and concentrated to provide a crude product, which was purified by silica column to afford compound **A14** as a white solid. Yield 54.6 %. ^{1}H NMR (600 MHz, DMSO-d_6) δ 7.84 (d, J = 8.4 Hz, 2H), 7.76 (d, J = 8.3 Hz, 2H), 7.71 (d, J = 7.4 Hz, 2H), 7.69–7.62 (m, 3H), 7.55–7.48 (m, 5H), 7.42 (t, J = 7.4 Hz, 1H), 7.14 (s, 1H), 6.76 (s, 1H), 4.69 (d, J = 10.1 Hz, 1H), 4.59 (d, J = 14.2 Hz, 1H), 4.36–4.29 (m, 2H). ^{13}C NMR (150 MHz, DMSO-d_6) δ 165.66 (s), 143.92 (s), 138.92 (s), 138.74 (s), 132.54 (t, J = 25.7 Hz), 130.70 (s), 129.08 (s, 2C), 128.75 (s), 128.30 (s), 127.84 (s), 127.01 (s), 126.91 (s, 2C), 126.68 (t, J = 6.4 Hz), 124.81 (s), 121.55 (t, J = 250.3 Hz), 120.99 (s), 79.00 (t, J = 27.5 Hz), 69.05 (s), 48.10 (s). HRMS (ESI, *m/z*) calcd for $C_{26}H_{21}F_2N_3O$, $[M+H]^+$, 430.1725; found 430.1727.

5.31. General procedure for the synthesis of intermediates ***48a-f***

$NaNO_2$ (1.5 equiv.) and urea (2.0 equiv.) were added to DMF, and then the mixture was cooled to −10 °C. Benzyl bromide (1.0 equiv.) was slowly dropwise added to the reaction, and the mixture was stirred for approximately 1 h. The reaction was poured into ice water and extracted with ether three times. The combined organic phase was concentrated *in vacuo* to afford the crude product, which was used directly for the next step without purification.

5.32. General procedure for the synthesis of intermediates ***49a-f***

To a solution of intermediate **48a-f** (1.0 equiv.) in alcohol and 1,4-dioxane, aqueous formaldehyde (20.0 equiv.) and NaOH (0.05 equiv.) were added. The resulting solution was stirred at room temperature for 1 h. The organic layer was evaporated *in vacuo*, and the residues were dissolved in water. The mixture was extracted with ethyl acetate three times. The combined organic extracts were dried and concentrated under reduced pressure to provide crude product, which was purified by silica gel chromatography to provide **49a-f** as a white solid.

*2-nitro-2-phenylpropane-1,3-diol (**49a**).*

^{1}H NMR (400 MHz, DMSO-d_6) δ 7.48–7.20 (m, 5H), 5.34 (t, J = 5.1 Hz, 2H), 4.37–4.12 (m, 4H).

5.33. General procedure for the synthesis of intermediates ***50a-f***

To a solution of intermediate **49a-f** (1.0 equiv.) and p-toluene sulfonic acid (0.01 equiv.) in acetone was added 2,2-dimethoxypropane (1.1 equiv.). The mixture was stirred at room temperature for 3 h and then quenched with Et_3N (0.2 equiv.). The organic layer was removed under reduced pressure and the residue was purified by silica gel chromatography to provide **50a-f** as colourless oil liquid.

*2,2-dimethyl-5-nitro-5-phenyl-1,3-dioxane (**50a**).*

^{1}H NMR (400 MHz, DMSO-d_6) δ 7.55–7.37 (m, 2H), 4.96 (dt, J = 3.2, 1.8 Hz, 1H), 4.41 (dt, J = 3.1, 1.8 Hz, 1H), 1.49 (s, 1H), 1.29 (s, 1H).

5.34. General procedure for the synthesis of intermediates ***51a-f***

To a solution of intermediate **50a-f** (1.0 equiv.) in ethanol, Raney Nickel (2.5 equiv, suspended in water) was added, and then H_2 was continuously bubbled in the reaction at room temperature for 18 h. After filtration, the filtrate was concentrated *in vacuo* to afford **51a-f** as colourless oil liquid.

*2,2-dimethyl-5-phenyl-1,3-dioxan-5-amine (**51a**).*

^{1}H NMR (400 MHz, DMSO-d_6) δ 7.62 (dt, J = 3.3, 1.9 Hz, 1H), 7.37–7.30 (m, 1H), 7.29–7.21 (m, 1H), 4.05 (d, J = 11.4 Hz, 1H), 3.53 (d, J = 11.4 Hz, 1H), 2.15 (s, 1H), 1.41 (d, J = 3.8 Hz, 1H).

5.35. General procedure for the synthesis of intermediates ***52a-y***

Intermediates **52a-y** were prepared in a similar manner as that for the intermediate **10**, using **51a-f** instead of **9**.

*N-(2,2-dimethyl-5-phenyl-1,3-dioxan-5-yl)-[1,1′-biphenyl]-4-carboxamide (**52a**).*

^{1}H NMR (400 MHz, DMSO-d_6) δ 8.58 (s, 1H), 8.00 (d, J = 8.3 Hz, 2H), 7.80 (d, J = 8.4 Hz, 2H), 7.78–7.70 (m, 2H), 7.55–7.47 (m, 4H), 7.42 (t, J = 7.3 Hz, 1H), 7.35 (t, J = 7.6 Hz, 2H), 7.26 (t, J = 7.3 Hz, 1H), 4.35 (d, J = 11.8 Hz, 2H), 4.21 (d, J = 11.8 Hz, 2H), 1.43 (d, J = 19.8 Hz, 6H).

5.36. General procedure for the synthesis of intermediates ***53a-y***

Intermediates **52a-f** were dissolved in a solution of glacial acetic acid and water (V:V = 3:1), and the reaction mixture was stirred at 60 °C for 1 h. Then the glacial acetic acid was removed under reduced pressure and the residue was dissolved in ethyl acetate. The organic phase was washed with water three times, dried with anhydrous Na_2SO_4 and concentrated with a vacuum to provide title intermediates 53a-y as a white solid.

*N-(1,3-dihydroxy-2-phenylpropan-2-yl)-[1,1′-biphenyl]-4-carboxamide (**53a**).*

^{1}H NMR (400 MHz, DMSO-d_6) δ 7.97 (d, J = 8.3 Hz, 1H), 7.84–7.76 (m, 1H), 7.77–7.71 (m, 1H), 7.56–7.47 (m, 1H), 7.45–7.35 (m, 1H), 7.33–7.25 (m, 1H), 7.24–7.14 (m, 1H), 4.99 (t, J = 5.9 Hz, 1H), 3.98 (d, J = 5.9 Hz, 1H).

5.37. General procedure for the synthesis of intermediates ***54a-y***

To a mixture of intermediates **53a-y** (1.0 equiv.), TsCl (3.0 equiv.) and DMAP (0.2 equiv.) in DCM, triethylamine (4.0 equiv.) was added at 0 °C. The reaction was stirred overnight and quenched with water. The reaction mixture was washed with citric acid (10 %) and saturated with $NaHCO_3$. The organic phase was dried and concentrated to provide a crude product, which was purified by silica gel chromatography to afford intermediates **54a-y** as a white solid.

*(2-([1,1′-biphenyl]-4-yl)-4-phenyl-4,5-dihydrooxazol-4-yl)methyl 4-methylbenzenesulfonate (**54a**).*

^{1}H NMR (400 MHz, DMSO) δ 7.96 (d, J = 8.5 Hz, 2H), 7.82 (d, J = 8.5 Hz, 2H), 7.78–7.74 (m, 2H), 7.66 (d, J = 8.3 Hz, 2H), 7.52 (t, J = 7.5 Hz, 2H), 7.48–7.41 (m, 3H), 7.40–7.29 (m, 5H), 4.81 (d, J = 9.1 Hz, 1H), 4.41 (d, J = 9.1 Hz, 1H), 4.36 (d, J = 9.9 Hz, 1H), 4.22 (d, J = 9.8 Hz, 1H), 2.37 (s, 3H).

5.38. The procedure for the synthesis of the compounds ***A15-A40***

Under an argon atmosphere, imidazole (triazole or tetrazole, 2 equiv.) and NaH (3 equiv.) were added to dry DMF at 0 °C. The reaction was stirred for 1 h. Then, intermediates **54a-y** (1 equiv.) were added, and the reaction was stirred at 80 °C for 12 h and controlled by TLC. The reaction was quenched with water and extracted with ethyl acetate three times. The combined organic layers were dried

over Na_2SO_4 and evaporated with a vacuum. The crude product was purified by silica gel column chromatography (CH_2Cl_2:CH_3OH = 40:1) to afford compounds **A15-A40**.

4-((1H-imidazole-1-yl*)methyl)-2-([1,1′-biphenyl]*-4-yl*)-4-phenyl-4,5-dihydrooxazole* (**A15**).

Light white solid; yield: 51.3 %; mp: 133.8–136.1 °C. ^{1}H NMR (600 MHz, DMSO-d_6) δ 7.99 (d, J = 8.4 Hz, 2H), 7.81 (d, J = 8.4 Hz, 2H), 7.74 (d, J = 7.2 Hz, 2H), 7.55–7.49 (m, 5H), 7.44–7.39 (m, 3H), 7.32 (t, J = 7.3 Hz, 1H), 7.09 (s, 1H), 6.75 (s, 1H), 4.82 (d, J = 9.1 Hz, 1H), 4.52 (d, J = 14.2 Hz, 1H), 4.43 (d, J = 9.1 Hz, 1H), 4.35 (d, J = 14.2 Hz, 1H). ^{13}C NMR (150 MHz, DMSO-d_6) δ 163.45 (s), 144.18 (s), 143.89 (s), 139.53 (s), 138.74 (s), 129.57 (s, 2C), 129.19 (s, 2C), 129.01 (s, 2C), 128.70 (s), 128.04 (s), 127.98 (s), 127.41 (s, 2C), 127.36 (s, 2C), 126.40 (s, 2C), 126.32 (s), 121.18 (s), 77.17 (s), 75.80 (s), 55.59 (s). HRMS (ESI, *m/z*) calcd for $C_{25}H_{21}N_3O$, $[M+H]^+$, 380.1757; found 380.1796.

4-((4H-1,2,4-triazol-1-yl*)methyl)-2-([1,1′-biphenyl]*-4-yl*)-4-phenyl-4,5-dihydrooxazole* (**A16**).

Light white solid; yield: 45.3 %; mp: 145.5–146.5 °C. ^{1}H NMR (600 MHz, DMSO-d_6) δ 8.32 (s, 1H), 7.96 (d, J = 8.4 Hz, 2H), 7.90 (s, 1H), 7.79 (d, J = 8.3 Hz, 2H), 7.73 (d, J = 7.5 Hz, 2H), 7.53–7.49 (m, 4H), 7.44–7.39 (m, 3H), 7.32 (t, J = 7.3 Hz, 1H), 5.13 (d, J = 8.9 Hz, 1H), 4.74 (d, J = 14.2 Hz, 1H), 4.61 (d, J = 14.1 Hz, 1H), 4.46 (d, J = 8.9 Hz, 1H). ^{13}C NMR (150 MHz, DMSO-d_6) δ 163.67 (s), 151.57 (s), 145.77 (s), 143.94 (s), 143.66 (s), 139.51 (s), 129.56 (s, 2C), 129.19 (s, 2C), 129.06 (s, 2C), 128.71 (s), 128.10 (s), 127.37 (s, 4C), 126.35 (s, 2C), 126.11 (s), 76.65 (s), 75.90 (s), 57.68 (s). HRMS (ESI, *m/z*) calcd for $C_{24}H_{20}N_4O$, $[M+Na]^+$, 403.1529; found 403.1563.

4-((1H-tetrazol-1-yl*)methyl)-2-([1,1′-biphenyl]*-4-yl*)-4-phenyl-4,5-dihydrooxazole* (**A17**).

Light white solid; yield: 31.3 %; mp: 178.6–180.4 °C. ^{1}H NMR (600 MHz, DMSO-d_6) δ 9.26 (s, 1H), 7.98 (d, J = 8.5 Hz, 2H), 7.81 (d, J = 8.5 Hz, 2H), 7.75–7.73 (m, 2H), 7.54–7.50 (m, 4H), 7.44–7.39 (m, 3H), 7.33 (t, J = 7.3 Hz, 1H), 5.08 (d, J = 14.2 Hz, 1H), 5.03 (d, J = 9.2 Hz, 1H), 4.96 (d, J = 14.2 Hz, 1H), 4.49 (d, J = 9.2 Hz, 1H). ^{13}C NMR (150 MHz, DMSO-d_6) δ 164.06 (s), 145.39 (s), 144.12 (s), 142.93 (s), 139.47 (s), 129.57 (s, 3C), 129.32 (s, 2C), 129.13 (s, 2C), 128.75 (s), 128.30 (s), 127.39 (s, 3C), 126.38 (s, 2C), 125.84 (s), 76.22 (s), 76.18 (s), 56.37 (s). HRMS (ESI, *m/z*) calcd for $C_{23}H_{19}N_5O$, $[M+Na]^+$, 404.1482; found 404.1514.

4-((1H-1,2,4-triazol-1-yl*)methyl)-2-(2-fluoro-[1,1′-biphenyl]*-4-yl*)-4-phenyl-4,5-dihydrooxazole* (**A18**).

Light white solid; yield: 42.5 %. ^{1}H NMR (600 MHz, DMSO-d_6) δ 8.37 (s, 1H), 7.91 (s, 1H), 7.78 (dd, J = 8.0, 1.6 Hz, 1H), 7.74 (dd, J = 11.2, 1.5 Hz, 1H), 7.67 (t, J = 8.0 Hz, 1H), 7.62–7.59 (m, 2H), 7.54–7.51 (m, 4H), 7.46 (t, J = 7.4 Hz, 1H), 7.41 (t, J = 7.6 Hz, 2H), 7.34 (t, J = 7.3 Hz, 1H), 5.16 (d, J = 9.0 Hz, 1H), 4.75 (d, J = 14.2 Hz, 1H), 4.62 (d, J = 14.2 Hz, 1H), 4.48 (d, J = 9.0 Hz, 1H). ^{13}C NMR (150 MHz, DMSO-d_6) δ 162.68 (s), 159.14 (d, J = 247.1 Hz), 151.61 (s), 145.86 (s), 143.42 (s), 134.60 (s), 132.19 (d, J = 13.1 Hz), 131.79 (s), 129.33 (s), 129.31 (s), 129.23 (s), 129.10 (s), 129.01 (s), 128.22 (d, J = 8.3 Hz), 128.17 (s), 126.34 (s), 125.03 (s), 116.04 (d, J = 25.4 Hz), 76.74 (s), 76.18 (s), 57.60 (s). HRMS (ESI, *m/z*) calcd for $C_{24}H_{19}FN_4O$, $[M+Na]^+$, 421.1435; found 421.1468.

4-((1H-1,2,4-triazol-1-yl*)methyl)-2-(3-fluoro-[1,1′-biphenyl]*-4-yl*)-4-phenyl-4,5-dihydrooxazole* (**A19**).

Light white solid; yield: 48.6 %; mp: 50.1–50.8 °C. ^{1}H NMR (600 MHz, DMSO-d_6) δ 8.35 (s, 1H), 7.92 (s, 1H), 7.89 (t, J = 7.9 Hz, 1H), 7.80–7.78 (m, 2H), 7.69 (dd, J = 12.3, 1.6 Hz, 1H), 7.65 (dd, J = 8.2, 1.7 Hz, 1H), 7.54–7.50 (m, 4H), 7.46 (t, J = 7.3 Hz, 1H), 7.41 (t, J = 7.7 Hz, 2H), 7.34 (t, J = 7.3 Hz, 1H), 5.13 (d, J = 9.0 Hz, 1H), 4.75 (d, J = 14.2 Hz, 1H), 4.63 (d, J = 14.1 Hz, 1H), 4.44 (d, J = 9.0 Hz, 1H). ^{13}C NMR (150 MHz, DMSO-d_6) δ 160.78 (d, J = 256.9 Hz), 160.29 (d, J = 4.9 Hz), 151.17 (s), 145.73 (d, J = 8.4 Hz), 145.35 (s), 143.01 (s), 137.64 (s), 131.59 (s), 129.17 (s, 2C), 128.90 (s), 128.65 (s, 2C), 127.72 (s), 127.03 (s, 2C), 125.90 (s, 2C), 122.66 (d, J = 2.8 Hz), 114.69 (d, J = 22.5 Hz), 113.63 (d, J = 10.9 Hz), 76.29 (s), 75.15 (s), 57.13 (s). HRMS (ESI, *m/z*) calcd for $C_{24}H_{19}FN_4O$, $[M+Na]^+$, 421.1435; found 421.1479.

4-((1H-1,2,4-triazol-1-yl*)methyl)-2-(2′-fluoro-[1,1′-biphenyl]*-4-yl*)-4-phenyl-4,5-dihydrooxazole* (**A20**).

Light white solid; yield: 35.2 %. ^{1}H NMR (600 MHz, DMSO-d_6) δ 8.33 (s, 1H), 7.97 (d, J = 8.4 Hz, 2H), 7.90 (s, 1H), 7.68 (dd, J = 8.3, 1.4 Hz, 2H), 7.59 (td, J = 7.9, 1.6 Hz, 1H), 7.53 (dd, J = 8.2, 1.1 Hz, 2H), 7.50–7.46 (m, 1H), 7.40 (t, J = 7.7 Hz, 2H), 7.37–7.31 (m, 3H), 5.14 (d, J = 8.9 Hz, 1H), 4.74 (d, J = 14.2 Hz, 1H), 4.62 (d, J = 14.1 Hz, 1H), 4.46 (d, J = 8.9 Hz, 1H). ^{13}C NMR (150 MHz, DMSO-d_6) δ 163.12 (s), 159.08 (d, J = 247.0 Hz), 151.12 (s), 145.33 (s), 143.16 (s), 138.51 (s), 130.80 (d, J = 2.4 Hz), 130.34 (d, J = 8.5 Hz), 129.11 (s, 2C), 128.61 (s, 2C), 128.35 (s, 2C), 127.65 (s), 127.26 (d, J = 12.9 Hz), 126.05 (s), 125.88 (s, 2C), 125.12 (d, J = 3.5 Hz), 116.26 (d, J = 22.6 Hz), 76.20 (s), 75.50 (s), 57.18 (s). HRMS (ESI, *m/z*) calcd for $C_{24}H_{19}FN_4O$, $[M+Na]^+$, 421.1435; found 421.1475.

4-((1H-1,2,4-triazol-1-yl*)methyl)-2-(3′-fluoro-[1,1′-biphenyl]*-4-yl*)-4-phenyl-4,5-dihydrooxazole* (**A21**).

Light white solid; yield: 50.2 %; mp: 105.4–107.0 °C. ^{1}H NMR (600 MHz, DMSO-d_6) δ 8.32 (s, 1H), 7.96 (d, J = 8.5 Hz, 2H), 7.90 (s, 1H), 7.84 (d, J = 8.5 Hz, 2H), 7.62–7.59 (m, 2H), 7.57–7.51 (m, 3H), 7.40 (t, J = 7.7 Hz, 2H), 7.33 (t, J = 7.3 Hz, 1H), 7.28–7.23 (m, 1H), 5.14 (d, J = 8.9 Hz, 1H), 4.74 (d, J = 14.2 Hz, 1H), 4.61 (d, J = 14.1 Hz, 1H), 4.46 (d, J = 8.9 Hz, 1H). ^{13}C NMR (150 MHz, DMSO-d_6) δ 163.57 (s), 163.18 (d, J = 243.3 Hz), 151.57 (s), 145.78 (s), 143.62 (s), 142.46 (s), 141.93 (d, J = 7.8 Hz), 131.52 (d, J = 8.6 Hz), 129.19 (s, 2C), 129.07 (s, 2C), 128.11 (s), 127.57 (s, 2C), 126.68 (s), 126.35 (s, 2C), 123.47 (d, J = 2.1 Hz), 115.43 (d, J = 21.0 Hz), 114.13 (d, J = 22.2 Hz), 76.67 (s), 75.93 (s), 57.67 (s). HRMS (ESI, *m/z*) calcd for $C_{24}H_{19}FN_4O$, $[M+Na]^+$, 421.1435; found 421.1473.

4-((1H-1,2,4-triazol-1-yl*)methyl)-2-(4′-fluoro-[1,1′-biphenyl]*-4-yl*)-4-phenyl-4,5-dihydrooxazole* (**A22**).

Light white solid; yield: 60.2 %; mp: 119.7–121.5 °C. ^{1}H NMR (600 MHz, DMSO-d_6) δ 8.32 (s, 1H), 7.94 (d, J = 8.5 Hz, 2H), 7.90 (s, 1H), 7.80–7.76 (m, 4H), 7.54–7.51 (m, 2H), 7.40 (t, J = 7.7 Hz, 2H), 7.35–7.31 (m, 3H), 5.13 (d, J = 8.9 Hz, 1H), 4.74 (d, J = 14.2 Hz, 1H), 4.61 (d, J = 14.1 Hz, 1H), 4.45 (d, J = 8.9 Hz, 1H). ^{13}C NMR (150 MHz, DMSO-d_6) δ 163.19 (s), 162.33 (d, J = 245.5 Hz), 151.11 (s), 145.31 (s), 143.18 (s), 142.42 (s), 135.53 (d, J = 3.0 Hz), 129.01 (d, J = 8.5 Hz, 2C), 128.74 (s, 2C), 128.62 (s, 2C), 127.65 (s), 126.87 (s, 2C), 125.89 (s, 2C), 125.63 (s), 115.94 (d, J = 21.6 Hz, 2C), 76.19 (s), 75.45 (s), 57.23 (s). HRMS (ESI, *m/z*) calcd for $C_{24}H_{19}FN_4O$, $[M+Na]^+$, 421.1435; found 421.1479.

4-((1H-1,2,4-triazol-1-yl*)methyl)-2-(3′,5′-difluoro-[1,1′-biphenyl]*-4-yl*)-4-phenyl-4,5-dihydrooxazole* (**A23**).

Light white solid; yield: 41.9 %; mp: 103.1–105.4 °C. ^{1}H NMR (600 MHz, DMSO-d_6) δ 8.33 (s, 1H), 7.96 (d, J = 8.5 Hz, 2H), 7.91–7.86 (m, 3H), 7.55–7.51 (m, 4H), 7.41 (t, J = 7.7 Hz, 2H), 7.35–7.28 (m, 2H), 5.15 (d, J = 8.9 Hz, 1H), 4.74 (d, J = 14.2 Hz, 1H), 4.61 (d, J = 14.1 Hz, 1H), 4.47 (d, J = 8.9 Hz, 1H). ^{13}C NMR (150 MHz, DMSO-d_6) δ 163.46 (s), 163.41 (d, J = 245.9 Hz), 163.32 (d, J = 246.1 Hz), 151.57 (s), 145.79 (s), 143.58 (s), 143.08 (t, J = 9.8 Hz), 141.23 (s), 129.17 (s, 2C), 129.08 (s, 2C), 128.13 (s), 127.70 (s, 2C), 127.22 (s), 126.34 (s, 2C), 110.68 (d, J = 5.3 Hz), 110.54 (d, J = 5.2 Hz), 103.97 (t, J = 25.9 Hz), 76.69 (s), 75.96 (s), 57.66 (s). HRMS (ESI, *m/z*) calcd for $C_{24}H_{18}F_2N_4O$, $[M+Na]^+$, 439.1341; found 439.1375.

4-((1H-1,2,4-triazol-1-yl*)methyl)-2-(2′-chloro-[1,1′-biphenyl]*-4-yl*)-4-phenyl-4,5-dihydrooxazole* (**A24**).

Light white solid; yield: 39.8 %. ^{1}H NMR (600 MHz, DMSO-d_6) δ 8.34 (s, 1H), 7.98–7.95 (m, 2H), 7.91 (s, 1H), 7.62–7.59 (m, 1H), 7.57–7.55 (m, 2H), 7.53–7.51 (m, 2H), 7.47–7.44 (m, 3H), 7.40 (t, J = 7.7 Hz, 2H), 7.33 (t, J = 7.3 Hz, 1H), 5.14 (d, J = 9.0 Hz, 1H), 4.75 (d, J = 14.2 Hz, 1H), 4.63 (d, J = 14.1 Hz, 1H), 4.47 (d, J = 9.0 Hz, 1H). ^{13}C

NMR (150 MHz, DMSO-d_6) δ 163.14 (s), 151.12 (s), 145.33 (s), 143.19 (s), 142.13 (s), 138.87 (s), 131.42 (s), 131.16 (s), 129.97 (s), 129.76 (s), 129.62 (s, 2C), 128.60 (s, 2C), 127.99 (s, 2C), 127.67 (s), 127.64 (s), 126.06 (s), 125.87 (s, 2C), 76.18 (s), 75.56 (s), 57.13 (s). HRMS (ESI, *m/z*) calcd for $C_{24}H_{19}ClN_4O$, $[M+Na]^+$, 437.1140; found 437.1177.

4-((1H-1,2,4-triazol-1-yl*)methyl)-2-(3′-chloro-[1,1′-biphenyl]*-4-yl*)-4-phenyl-4,5-dihydrooxazole* (**A25**).

Light white solid; yield: 42.5 %. ^{1}H NMR (600 MHz, DMSO-d_6) δ 8.32 (s, 1H), 7.96 (d, J = 8.5 Hz, 2H), 7.90 (s, 1H), 7.84 (d, J = 8.4 Hz, 2H), 7.81 (t, J = 1.8 Hz, 1H), 7.73–7.71 (m, 1H), 7.55–7.48 (m, 4H), 7.41 (t, J = 7.7 Hz, 2H), 7.33 (t, J = 7.3 Hz, 1H), 5.14 (d, J = 8.9 Hz, 1H), 4.74 (d, J = 14.2 Hz, 1H), 4.61 (d, J = 14.1 Hz, 1H), 4.46 (d, J = 8.9 Hz, 1H). ^{13}C NMR (150 MHz, DMSO-d_6) δ 163.11 (s), 151.12 (s), 145.33 (s), 143.16 (s), 141.85 (s), 141.19 (s), 133.91 (s), 130.94 (s), 128.76 (s, 2C), 128.63 (s, 2C), 128.07 (s), 127.67 (s), 127.16 (s, 2C), 126.66 (s), 126.25 (s), 125.90 (s, 2C), 125.66 (s), 76.23 (s), 75.48 (s), 57.22 (s). HRMS (ESI, *m/z*) calcd for $C_{24}H_{19}ClN_4O$, $[M+Na]^+$, 437.1140; found 437.1170.

4-((1H-1,2,4-triazol-1-yl*)methyl)-2-(4′-chloro-[1,1′-biphenyl]*-4-yl*)-4-phenyl-4,5-dihydrooxazole* (**A26**).

Light white solid; yield: 50.7 %; mp: 156.1–156.8 °C. ^{1}H NMR (600 MHz, DMSO-d_6) δ 8.32 (s, 1H), 7.95 (d, J = 8.5 Hz, 2H), 7.89 (s, 1H), 7.80 (d, J = 8.5 Hz, 2H), 7.77 (d, J = 8.6 Hz, 2H), 7.56 (d, J = 8.6 Hz, 2H), 7.53–7.51 (m, 2H), 7.40 (t, J = 7.7 Hz, 2H), 7.32 (t, J = 7.3 Hz, 1H), 5.14 (d, J = 8.9 Hz, 1H), 4.74 (d, J = 14.2 Hz, 1H), 4.61 (d, J = 14.1 Hz, 1H), 4.46 (d, J = 8.9 Hz, 1H). ^{13}C NMR (150 MHz, DMSO-d_6) δ 163.58 (s), 151.57 (s), 145.77 (s), 143.63 (s), 142.55 (s), 138.30 (s), 133.63 (s), 129.52 (s, 2C), 129.24 (s, 2C), 129.16 (s, 2C), 129.07 (s, 2C), 128.11 (s), 127.36 (s, 2C), 126.43 (s), 126.35 (s, 2C), 76.67 (s), 75.92 (s), 57.68 (s). HRMS (ESI, *m/z*) calcd for $C_{24}H_{19}ClN_4O$, $[M+Na]^+$, 437.1140; found 437.1182.

4′-(4-((1H-1,2,4-triazol-1-yl*)methyl)-4-phenyl-4,5-dihydrooxazol*-2-yl*)-[1,1′-biphenyl]-4-carbonitrile* (**A27**).

Light white solid; yield: 38.3 %; mp: 157.1–159.1 °C. ^{1}H NMR (600 MHz, DMSO-d_6) δ 8.32 (s, 1H), 8.00–7.94 (m, 6H), 7.90–7.86 (m, 3H), 7.53 (dd, J = 8.2, 1.1 Hz, 2H), 7.40 (t, J = 7.7 Hz, 2H), 7.33 (t, J = 7.3 Hz, 1H), 5.15 (d, J = 8.9 Hz, 1H), 4.74 (d, J = 14.2 Hz, 1H), 4.61 (d, J = 14.2 Hz, 1H), 4.47 (d, J = 8.9 Hz, 1H). ^{13}C NMR (150 MHz, DMSO-d_6) δ 161.39 (s), 149.50 (s), 143.71 (s), 141.88 (s), 141.51 (s), 139.87 (s), 131.37 (s, 2C), 127.22 (s, 2C), 127.00 (s, 2C), 126.23 (s, 2C), 126.05 (s), 125.82 (s, 2C), 125.20 (s), 124.27 (s, 2C), 117.14 (s), 109.16 (s), 74.63 (s), 73.90 (s), 55.58 (s). HRMS (ESI, *m/z*) calcd for $C_{25}H_{19}N_5O$, $[M+Na]^+$, 428.1482; found 428.1527.

4-((1H-1,2,4-triazol-1-yl*)methyl)-4-phenyl-2-(4′-(trifluoromethoxy)-[1,1′-biphenyl]*-4-yl*)-4,5-dihydrooxazole* (**A28**).

Light white solid; yield: 41.5 %; mp: 117.1–118.7 °C. ^{1}H NMR (600 MHz, DMSO-d_6) δ 8.32 (s, 1H), 7.96 (d, J = 8.5 Hz, 2H), 7.90 (s, 1H), 7.87 (d, J = 8.8 Hz, 2H), 7.81 (d, J = 8.5 Hz, 2H), 7.52 (dd, J = 8.3, 1.1 Hz, 2H), 7.50 (d, J = 8.1 Hz, 2H), 7.40 (t, J = 7.7 Hz, 2H), 7.33 (t, J = 7.3 Hz, 1H), 5.14 (d, J = 8.9 Hz, 1H), 4.74 (d, J = 14.2 Hz, 1H), 4.61 (d, J = 14.2 Hz, 1H), 4.46 (d, J = 8.9 Hz, 1H). ^{13}C NMR (150 MHz, DMSO-d_6) δ 163.10 (s), 151.10 (s), 148.35 (s), 145.31 (s), 143.16 (s), 141.96 (s), 138.35 (s), 128.89 (s, 2C), 128.76 (s, 2C), 128.59 (s, 2C), 127.64 (s), 127.09 (s, 2C), 126.05 (s), 125.88 (s, 2C), 121.57 (s, 2C), 120.10 (dd, J = 513.1, 256.6 Hz), 76.19 (s), 75.47 (s), 57.19 (s). HRMS (ESI, *m/z*) calcd for $C_{25}H_{19}F_3N_4O_2$, $[M+Na]^+$, 487.1352; found 487.1380.

4-((1H-1,2,4-triazol-1-yl*)methyl)-4-phenyl-2-(4′-(trifluoromethyl)-[1,1′-biphenyl]*-4-yl*)-4,5-dihydrooxazole* (**A29**).

Light white solid; yield: 54.2 %; mp: 116.8–119.0 °C. ^{1}H NMR (600 MHz, DMSO-d_6) δ 8.38 (s, 1H), 8.05 (d, J = 8.5 Hz, 2H), 8.02 (d, J = 8.2 Hz, 2H), 7.95 (s, 1H), 7.92 (dd, J = 8.1, 5.9 Hz, 4H), 7.59 (dd, J = 8.2, 1.1 Hz, 2H), 7.46 (t, J = 7.7 Hz, 2H), 7.38 (t, J = 7.3 Hz, 1H), 5.20 (d, J = 8.9 Hz, 1H), 4.80 (d, J = 14.2 Hz, 1H), 4.67 (d, J = 14.2 Hz, 1H), 4.52 (d, J = 8.9 Hz, 1H). ^{13}C NMR (150 MHz, DMSO-d_6) δ 163.52 (s), 151.58 (s), 145.78 (s), 143.59 (s), 143.51 (s), 142.28 (s), 129.30 (s, 2C), 129.08 (s, 2C), 128.24 (s, 3C), 128.12 (s), 127.84 (s, 2C), 127.05 (s), 126.40 (s), 126.37 (s), 126.35 (s, 2C), 124.75 (q, J = 272.1 Hz), 76.70 (s), 75.96 (s), 57.66 (s). HRMS (ESI, *m/z*) calcd for $C_{25}H_{19}F_3N_4O$, $[M+Na]^+$, 471.1403; found 471.1437.

4-((1H-1,2,4-triazol-1-yl*)methyl)-2-(2′-fluoro-[1,1′-biphenyl]*-4-yl*)-4-(3-fluorophenyl)-4,5-dihydrooxazole* (**A30**).

Light white solid; yield: 43.4 %; mp: 100.4–102.1 °C. ^{1}H NMR (600 MHz, DMSO-d_6) δ 8.35 (s, 1H), 7.98 (d, J = 8.4 Hz, 2H), 7.90 (s, 1H), 7.68 (dd, J = 8.2, 1.2 Hz, 2H), 7.59 (td, J = 7.9, 1.5 Hz, 1H), 7.50–7.43 (m, 2H), 7.39–7.33 (m, 4H), 7.16 (td, J = 8.3, 2.1 Hz, 1H), 5.13 (d, J = 9.1 Hz, 1H), 4.77 (d, J = 14.1 Hz, 1H), 4.64 (d, J = 14.1 Hz, 1H), 4.48 (d, J = 9.1 Hz, 1H). ^{13}C NMR (150 MHz, DMSO-d_6) δ 163.45 (s), 162.18 (d, J = 243.4 Hz), 159.07 (d, J = 247.0 Hz), 151.14 (s), 145.92 (d, J = 6.7 Hz), 145.39 (s), 138.61 (s), 130.79 (d, J = 2.4 Hz), 130.63 (d, J = 8.0 Hz), 130.35 (d, J = 8.3 Hz), 129.11 (d, J = 2.3 Hz, 2C), 128.40 (s, 2C), 127.23 (d, J = 13.0 Hz), 125.91 (s), 125.12 (d, J = 3.5 Hz), 122.02 (s), 116.26 (d, J = 22.3 Hz), 114.49 (d, J = 20.9 Hz), 113.03 (d, J = 22.8 Hz), 75.95 (s), 75.43 (s), 56.90 (s). HRMS (ESI, *m/z*) calcd for $C_{24}H_{18}F_2N_4O$, $[M+Na]^+$, 439.1341; found 439.1387.

4-((1H-1,2,4-triazol-1-yl*)methyl)-2-(3′-fluoro-[1,1′-biphenyl]*-4-yl*)-4-(3-fluorophenyl)-4,5-dihydrooxazole* (**A31**).

Light white solid; yield: 46.5 %; mp: 128.6–130.4 °C. ^{1}H NMR (600 MHz, DMSO-d_6) δ 8.34 (s, 1H), 7.96 (d, J = 8.5 Hz, 2H), 7.89 (s, 1H), 7.84 (d, J = 8.5 Hz, 2H), 7.62–7.59 (m, 2H), 7.57–7.53 (m, 1H), 7.44 (td, J = 8.0, 6.2 Hz, 1H), 7.39–7.34 (m, 2H), 7.28–7.24 (m, 1H), 7.18–7.14 (m, 1H), 5.13 (d, J = 9.0 Hz, 1H), 4.77 (d, J = 14.2 Hz, 1H), 4.63 (d, J = 14.1 Hz, 1H), 4.48 (d, J = 9.0 Hz, 1H). ^{13}C NMR (150 MHz, DMSO-d_6) δ 163.43 (s), 163.25 (d, J = 80.8 Hz), 161.64 (d, J = 80.7 Hz), 151.13 (s), 145.91 (d, J = 6.8 Hz), 145.37 (s), 142.08 (s), 141.43 (d, J = 7.8 Hz), 131.05 (d, J = 8.8 Hz), 130.63 (d, J = 8.5 Hz), 128.77 (s, 2C), 127.11 (s, 2C), 126.07 (s), 123.01 (d, J = 2.1 Hz), 122.03 (d, J = 2.1 Hz), 114.98 (d, J = 21.3 Hz), 114.48 (d, J = 20.8 Hz), 113.67 (d, J = 22.5 Hz), 113.03 (d, J = 22.4 Hz), 75.96 (s), 75.39 (s), 56.93 (s). HRMS (ESI, *m/z*) calcd for $C_{24}H_{18}F_2N_4O$, $[M+Na]^+$, 439.1341; found 439.1371.

4-((1H-1,2,4-triazol-1-yl*)methyl)-4-(3-chlorophenyl)-2-(2′-fluoro-[1,1′-biphenyl]*-4-yl*)-4,5-dihydrooxazole* (**A32**).

Light white solid; yield: 54.3 %; mp: 102.7–103.6 °C. ^{1}H NMR (600 MHz, DMSO-d_6) δ 8.36 (s, 1H), 7.98 (d, J = 8.3 Hz, 2H), 7.90 (s, 1H), 7.71–7.66 (m, 2H), 7.62–7.57 (m, 2H), 7.50–7.46 (m, 2H), 7.43 (t, J = 7.7 Hz, 1H), 7.41–7.38 (m, 1H), 7.35 (dd, J = 15.5, 7.9 Hz, 2H), 5.14 (d, J = 9.1 Hz, 1H), 4.77 (d, J = 14.2 Hz, 1H), 4.64 (d, J = 14.1 Hz, 1H), 4.48 (d, J = 9.1 Hz, 1H). ^{13}C NMR (150 MHz, DMSO-d_6) δ 163.96 (s), 159.55 (d, J = 246.7 Hz), 151.61 (s), 145.97 (s), 145.87 (s), 139.10 (s), 133.77 (s), 131.25 (d, J = 2.8 Hz), 130.97 (s), 130.81 (d, J = 8.3 Hz), 129.58 (d, J = 2.8 Hz, 2C), 128.88 (s, 2C), 128.13 (s), 127.71 (d, J = 13.0 Hz), 126.43 (s), 126.38 (s), 125.58 (d, J = 3.5 Hz), 125.18 (s), 116.72 (d, J = 22.6 Hz), 76.41 (s), 75.87 (s), 57.41 (s). HRMS (ESI, *m/z*) calcd for $C_{24}H_{18}ClFN_4O$, $[M+Na]^+$, 455.1045; found 455.1079.

4-((1H-1,2,4-triazol-1-yl*)methyl)-2-(2′-fluoro-[1,1′-biphenyl]*-4-yl*)-4-(4-fluorophenyl)-4,5-dihydrooxazole* (**A33**).

Light white solid; yield: 35.1 %; mp: 122.5–1124.4 °C. ^{1}H NMR (600 MHz, DMSO-d_6) δ 8.34 (s, 1H), 7.98 (d, J = 8.3 Hz, 2H), 7.90 (s, 1H), 7.68 (d, J = 7.1 Hz, 2H), 7.59 (td, J = 7.9, 1.3 Hz, 1H), 7.56 (dd, J = 8.7, 5.5 Hz, 2H), 7.48 (ddd, J = 9.3, 7.2, 1.5 Hz, 1H), 7.35 (dd, J = 15.8, 8.3 Hz, 2H), 7.22 (t, J = 8.8 Hz, 2H), 5.13 (d, J = 9.0 Hz, 1H), 4.74 (d, J = 14.1 Hz, 1H), 4.61 (d, J = 14.1 Hz, 1H), 4.46 (d, J = 9.0 Hz, 1H). ^{13}C NMR (150 MHz, DMSO-d_6) δ δ 163.25 (s), 161.49 (d, J = 243.5 Hz), 159.07 (d, J = 246.5 Hz), 151.11 (s), 145.33 (s), 139.30 (s), 138.56 (s), 130.78 (d, J = 2.9 Hz), 130.33 (d, J = 8.2 Hz), 129.09 (d, J = 2.7 Hz, 2C), 128.37 (s, 2C), 128.04 (d, J = 8.4 Hz, 2C), 127.23 (d, J = 12.7 Hz), 125.97 (s), 125.11 (d, J = 3.3 Hz), 116.25 (d, J = 22.3 Hz), 115.30 (d, J = 21.2 Hz, 2C), 75.78 (s), 75.57 (s), 57.12 (s). HRMS (ESI, *m/z*) calcd for $C_{24}H_{18}F_2N_4O$, $[M+Na]^+$, 439.1341; found 439.1382. Retention time: 24.79 min, 98.70 % purity.

4-((1H-1,2,4-triazol-1-yl*)methyl)-2-(3′-fluoro-[1,1′-biphenyl]*-4-yl*)-4-(4-fluorophenyl)-4,5-dihydrooxazole* (**A34**).

Light white solid; yield: 38.6 %. ^{1}H NMR (600 MHz, DMSO-d_6) δ 8.33 (s, 1H), 7.96 (d, J = 8.5 Hz, 2H), 7.89 (s, 1H), 7.84 (d, J = 8.5 Hz, 2H), 7.62−7.59 (m, 2H), 7.57−7.53 (m, 3H), 7.28−7.20 (m, 3H), 5.13 (d, J = 9.0 Hz, 1H), 4.74 (d, J = 14.2 Hz, 1H), 4.61 (d, J = 14.1 Hz, 1H), 4.45 (d, J = 9.0 Hz, 1H). ^{13}C NMR (150 MHz, DMSO-d_6) δ 163.23 (s), 162.91 (d, J = 183.8 Hz), 161.30 (d, J = 184.4 Hz), 151.11 (s), 145.33 (s), 142.04 (d, J = 1.9 Hz), 141.43 (d, J = 7.8 Hz), 139.30 (d, J = 2.4 Hz), 131.05 (d, J = 8.6 Hz), 128.75 (s, 2C), 128.05 (d, J = 8.4 Hz, 2C), 127.10 (s, 2C), 126.13 (s), 123.00 (d, J = 2.1 Hz), 115.31 (d, J = 21.4 Hz, 2C), 114.97 (d, J = 21.1 Hz), 113.66 (d, J = 22.2 Hz), 75.79 (s), 75.54 (s), 57.15 (s). HRMS (ESI, *m/z*) calcd for $C_{24}H_{18}F_2N_4O$, $[M+Na]^+$, 439.1341; found 439.1390. Retention time: 10.46 min, 100 % purity.

4-((1H-1,2,4-triazol-1-yl*)methyl)-4-(4-chlorophenyl)-2-(2′-fluoro-[1,1′-biphenyl]*-4-yl*)-4,5-dihydrooxazole* (**A35**).

Light white solid; yield: 37.3 %; mp: 123.2−123.6 °C. ^{1}H NMR (600 MHz, DMSO-d_6) δ 8.35 (s, 1H), 7.98 (d, J = 8.4 Hz, 2H), 7.90 (s, 1H), 7.68 (dd, J = 8.3, 1.4 Hz, 2H), 7.61−7.58 (m, 1H), 7.54 (d, J = 8.6 Hz, 2H), 7.50−7.47 (m, 1H), 7.46 (d, J = 8.6 Hz, 2H), 7.34 (dd, J = 10.7, 4.4 Hz, 2H), 5.12 (d, J = 9.0 Hz, 1H), 4.75 (d, J = 14.2 Hz, 1H), 4.62 (d, J = 14.1 Hz, 1H), 4.45 (d, J = 9.0 Hz, 1H). ^{13}C NMR (150 MHz, DMSO-d_6) δ 163.35 (s), 159.07 (d, J = 247.0 Hz), 151.13 (s), 145.37 (s), 142.04 (s), 138.60 (s), 132.30 (s), 130.79 (d, J = 2.4 Hz), 130.35 (d, J = 8.5 Hz), 129.09 (s, 2C), 128.51 (s, 2C), 128.39 (s, 2C), 127.93 (s, 2C), 127.22 (d, J = 12.7 Hz), 125.92 (s), 125.12 (d, J = 3.3 Hz), 116.26 (d, J = 22.2 Hz), 75.84 (s), 75.46 (s), 56.95 (s). HRMS (ESI, *m/z*) calcd for $C_{24}H_{18}ClFN_4O$, $[M+Na]^+$, 455.1045; found 455.1093. Retention time: 25.32 min, 97.66 % purity.

4-((1H-1,2,4-triazol-1-yl*)methyl)-4-(4-chlorophenyl)-2-(3′-fluoro-[1,1′-biphenyl]*-4-yl*)-4,5-dihydrooxazole* (**A36**).

Light white solid; yield: 42.9 %; mp: 53.4−54.7 °C. ^{1}H NMR (600 MHz, DMSO-d_6) δ 8.34 (s, 1H), 7.96 (d, J = 8.4 Hz, 2H), 7.89 (s, 1H), 7.84 (d, J = 8.4 Hz, 2H), 7.61−7.59 (m, 2H), 7.55−7.52 (m, 3H), 7.46 (d, J = 8.6 Hz, 2H), 7.26 (td, J = 8.1, 1.5 Hz, 1H), 5.12 (d, J = 9.0 Hz, 1H), 4.74 (d, J = 14.2 Hz, 1H), 4.62 (d, J = 14.1 Hz, 1H), 4.45 (d, J = 9.0 Hz, 1H). ^{13}C NMR (150 MHz, DMSO-d_6) δ 163.34 (s), 162.71 (d, J = 243.4 Hz), 151.13 (s), 145.35 (s), 142.07 (s), 142.03 (s), 141.42 (d, J = 7.8 Hz), 132.30 (s), 131.05 (d, J = 8.3 Hz), 128.76 (s, 2C), 128.51 (s, 2C), 127.93 (s, 2C), 127.11 (s, 2C), 126.08 (s), 123.00 (d, J = 2.0 Hz), 114.98 (d, J = 21.0 Hz), 113.66 (d, J = 22.1 Hz), 75.84 (s), 75.43 (s), 56.98 (s). HRMS (ESI, *m/z*) calcd for $C_{24}H_{18}ClFN_4O$, $[M+Na]^+$, 455.1045; found 455.1083.

4-((1H-1,2,4-triazol-1-yl*)methyl)-4-(2,4-difluorophenyl)-2-(2′-fluoro-[1,1′-biphenyl]*-4-yl*)-4,5-dihydrooxazole* (**A37**).

Light white solid; yield: 56.4 %; mp: 129.2−130.5 °C. ^{1}H NMR (600 MHz, DMSO-d_6) δ 8.39 (s, 1H), 8.00 (d, J = 8.5 Hz, 2H), 7.87 (s, 1H), 7.72−7.68 (m, 3H), 7.60 (td, J = 7.9, 1.6 Hz, 1H), 7.50−7.46 (m, 1H), 7.39−7.33 (m, 3H), 7.11 (td, J = 8.5, 2.5 Hz, 1H), 5.15 (dd, J = 9.2, 2.5 Hz, 1H), 4.64 (d, J = 14.3 Hz, 1H), 4.58 (d, J = 14.3 Hz, 1H), 4.48 (dd, J = 9.1, 1.6 Hz, 1H). ^{13}C NMR (150 MHz, DMSO-d_6) δ 163.60 (s), 162.03 (dd, J = 246.8, 12.6 Hz), 159.89 (s), 159.26 (dd, J = 246.6, 12.4 Hz), 159.07 (d, J = 246.2 Hz), 151.06 (s), 145.32 (s), 138.76 (s), 130.80 (d, J = 2.4 Hz), 130.38 (d, J = 8.1 Hz), 129.45 (dd, J = 9.5, 6.3 Hz), 129.13 (d, J = 2.3 Hz, 2C), 128.50 (s, 2C), 127.20 (d, J = 12.9 Hz), 126.00 (dd, J = 14.1, 3.1 Hz), 125.75 (s), 125.13 (d, J = 3.5 Hz), 116.27 (d, J = 22.3 Hz), 111.58 (d, J = 20.9 Hz), 104.53 (t, J = 26.2 Hz), 74.90 (d, J = 7.1 Hz), 73.76 (d, J = 3.0 Hz), 55.89 (s). HRMS (ESI, *m/z*) calcd for $C_{24}H_{17}F_3N_4O$, $[M+Na]^+$, 457.1247; found 457.1282.

4-((1H-1,2,4-triazol-1-yl*)methyl)-4-(2,4-difluorophenyl)-2-(3′-fluoro-[1,1′-biphenyl]*-4-yl*)-4,5-dihydrooxazole* (**A38**).

Light white solid; yield: 58.3 %; mp: 149.6−150.4 °C. ^{1}H NMR (600 MHz, DMSO-d_6) δ 8.38 (s, 1H), 7.98 (d, J = 8.5 Hz, 2H), 7.88−7.84 (m, 3H), 7.71 (td, J = 8.7, 6.8 Hz, 1H), 7.63−7.60 (m, 2H), 7.55 (td, J = 8.1, 6.2 Hz, 1H), 7.40−7.35 (m, 1H), 7.29−7.25 (m, 1H), 7.11 (td, J = 8.5, 2.5 Hz, 1H), 5.14 (dd, J = 9.1, 2.5 Hz, 1H), 4.64 (d, J = 14.3 Hz, 1H), 4.58 (d, J = 14.3 Hz, 1H), 4.47 (dd, J = 9.1, 1.6 Hz, 1H). ^{13}C NMR (150 MHz, DMSO-d_6) δ 163.59 (s), 162.72 (d, J = 243.9 Hz), 162.03 (dd, J = 246.5, 12.4 Hz), 159.25 (dd, J = 246.5, 12.4 Hz), 151.06 (s), 145.31 (s), 142.22 (s), 141.39 (d, J = 7.8 Hz), 131.06 (d, J = 8.8 Hz), 129.46 (dd, J = 9.3, 6.3 Hz), 128.87 (s, 2C), 127.14 (s, 2C), 126.00 (dd, J = 14.3, 3.6 Hz), 125.90 (s), 123.02 (d, J = 1.8 Hz), 115.02 (d, J = 20.9 Hz), 113.69 (d, J = 22.5 Hz), 111.57 (d, J = 18.8 Hz), 104.53 (t, J = 26.1 Hz), 74.87 (d, J = 6.9 Hz), 73.76 (d, J = 2.5 Hz), 55.90 (s). HRMS (ESI, *m/z*) calcd for $C_{24}H_{17}F_3N_4O$, $[M+Na]^+$, 457.1247; found 457.1286. Retention time: 11.06 min, 98.27 % purity.

4-((1H-1,2,4-triazol-1-yl*)methyl)-4-(3,5-difluorophenyl)-2-(2′-fluoro-[1,1′-biphenyl]*-4-yl*)-4,5-dihydrooxazole* (**A39**).

Light white solid; yield: 40.6 %; mp: 114.6−116.4 °C. ^{1}H NMR (600 MHz, DMSO-d_6) δ 8.37 (s, 1H), 7.99 (d, J = 8.5 Hz, 2H), 7.90 (s, 1H), 7.69 (dd, J = 8.3, 1.4 Hz, 2H), 7.59 (td, J = 7.9, 1.6 Hz, 1H), 7.50−7.46 (m, 1H), 7.38−7.33 (m, 2H), 7.26 (dd, J = 8.6, 2.2 Hz, 2H), 7.21 (tt, J = 9.1, 2.3 Hz, 1H), 5.11 (d, J = 9.2 Hz, 1H), 4.79 (d, J = 14.2 Hz, 1H), 4.66 (d, J = 14.1 Hz, 1H), 4.50 (d, J = 9.2 Hz, 1H). ^{13}C NMR (150 MHz, DMSO-d_6) δ 163.78 (s), 162.40 (dd, J = 246.1, 13.1 Hz, 2C), 159.07 (d, J = 247.0 Hz), 151.17 (s), 147.48 (t, J = 8.8 Hz), 145.45 (s), 138.70 (s), 130.79 (d, J = 2.3 Hz), 130.37 (d, J = 8.3 Hz), 129.12 (d, J = 2.2 Hz, 2C), 128.47 (s, 2C), 127.21 (d, J = 13.0 Hz), 125.79 (s), 125.13 (d, J = 3.4 Hz), 116.26 (d, J = 22.7 Hz), 109.58 (d, J = 5.5 Hz), 109.44 (d, J = 5.3 Hz), 103.17 (t, J = 25.6 Hz), 75.91 (s), 75.31 (s), 56.66 (s). HRMS (ESI, *m/z*) calcd for $C_{24}H_{17}F_3N_4O$, $[M+Na]^+$, 457.1247; found 457.1281.

4-((1H-1,2,4-triazol-1-yl*)methyl)-4-(3,5-difluorophenyl)-2-(3′-fluoro-[1,1′-biphenyl]*-4-yl*)-4,5-dihydrooxazole* (**A40**).

Light white solid; yield: 52.6 %; mp: 143.1−146.8 °C. ^{1}H NMR (600 MHz, DMSO-d_6) δ 8.37 (s, 1H), 7.97 (d, J = 8.5 Hz, 2H), 7.90 (s, 1H), 7.84 (d, J = 8.5 Hz, 2H), 7.62−7.59 (m, 2H), 7.57−7.53 (m, 1H), 7.29−7.24 (m, 3H), 7.23−7.19 (m, 1H), 5.11 (d, J = 9.2 Hz, 1H), 4.79 (d, J = 14.2 Hz, 1H), 4.65 (d, J = 14.1 Hz, 1H), 4.50 (d, J = 9.2 Hz, 1H). ^{13}C NMR (150 MHz, DMSO-d_6) δ 163.76 (s), 162.71 (d, J = 243.3 Hz), 162.40 (dd, J = 246.1, 13.1 Hz, 2C), 151.17 (s), 147.47 (t, J = 8.9 Hz), 145.44 (s), 142.17 (s), 141.41 (d, J = 7.8 Hz), 131.05 (d, J = 8.8 Hz), 128.84 (s, 2C), 127.12 (s, 2C), 125.94 (s), 123.01 (d, J = 2.2 Hz), 115.00 (d, J = 21.1 Hz), 113.67 (d, J = 22.2 Hz), 109.58 (d, J = 5.4 Hz), 109.44 (d, J = 5.1 Hz), 103.17 (t, J = 25.9 Hz), 75.92 (s), 75.28 (s), 56.69 (s). HRMS (ESI, *m/z*) calcd for $C_{24}H_{17}F_3N_4O$, $[M+Na]^+$, 457.1247; found 457.1279.

5.39. In vitro antifungal testing

Five sensitive pathogenic fungi and two fluconazole-resistant strains of *Candida albicans* were selected to determine the *in vitro* minimum inhibitory concentrations (MICs) according to the protocols of the National Committee for Clinical Laboratory Standards (NCCLS). The MIC values were defined as the lowest concentrations of an antimicrobial that would inhibit the visible growth of the fungi. Fluconazole and itraconazole were used as positive control drugs. All of the compounds were dissolved in DMSO and serially diluted into the growth medium.

5.40. GC-MS analysis of sterol composition

Candida albicans (SC5314) was treated with compounds **A33** (0.015 μg/mL), **A34** (0.015 μg/mL) and fluconazole (0.25 μg/mL) at sub-MIC values and incubated in RPMI 1640 medium (50 mL) for ~18 h at 30 °C with continuous agitation (200 rpm). Cells were harvested by centrifugation at 3000*g* for 10 min. Then the cells were washed with PBS three times, and saponified at 80 °C for 60 min with 3 mL of ethanol, 2 mL of pyrogallol dissolved in

ethanol, and 2 mL of KOH (60 %, w/v). The nonsaponifiable sterols were extracted three times with 5 mL of heptane. The combined extracts were evaporated in a vacuum, and the residue was dissolved in 500 μL of heptane and derivatized with 250 μL of *N*-methyl-*N*-(trimethylsilyl) trifluorooacetaminde (MSTFA) at 70 °C for 20 min. The sterols were analysed by GC-MS. The GC-MS data were analysed using Agilent software (Agilent MSD productivity ChemStation for GC and GC/MS systems data analysis application) and matched to known MS data using the NIST Spectrum Database.

5.41. In vitro human liver microsomes stability assay

5 μL of the test sample (100 μM, 99 % acetonitrile) or reference drug (100 μM, 99 % acetonitrile) was mixed with 445 μL of liver microsome solution (0.56 mg/mL) and incubated in a 37 °C water bath with shaking for 10 min. Then, 44 μL of NAPDH cofactor was add to the incubated solution. At 5, 10, 20, 30, and 60 min, 180 μL of quenching solution was add to terminate the reactions. All quenched samples were shaken for 10 min and centrifuged at 4000 rpm for 20 min at 4 °C 80 μL of supernatant was mixed with 240 μL of ultrapure water and shaken for 10 min to prepare samples for LC-MS/MS analysis.

5.42. In vitro human plasma stability assay

Blank plasma (98 μL) was mixed with 2 μL of dosing solution (100 μM) to achieve a final concentration of 2 μM in duplicate, and samples were incubated at 37 °C in a water bath. At each time point (0, 10, 30, 60 and 120 min), 400 μL of stop solution (200 ng/mL tolbutamide and 200 ng/mL labetalol in 50 % ACN/MeOH) was added to terminate the reactions. The sample plates were centrifuged at 4000 rpm for approximately 10 min. The supernatant (50 μL) was mixed with 100 μL of ultrapure water. The samples were shaken at 800 rpm for 10 min. Samples were analysed by LC/MS/MS. The disappearance of test compounds was assessed based on the peak area ratio of analyte/IS (no standard curve).

5.43. Cytochrome P450 enzyme inhibition assay

20 μL of CYP substrate solution was added to the corresponding wells of the 96-well plate, and 2 μL of the test compound and CYP inhibitor were added. Then, 158 μL of human liver microsomal solution was added. The 96-well plate was prewarmed for approximately 10 min at 37 °C water bath. 20 μL of NADPH cofactor was added to all incubated wells. The samples were mixed and further incubated for 10 min at 37 °C. At this time point, the reaction was terminated by adding 400 μL of cold stop solution (200 ng/mL tolbutamide and labetalol in ACN). The sample solution was centrifuged at 4000 rpm for 20 min, and 200 μL of supernatant was mixed with 100 μL of ultrapure water by shock for 10 min to prepare LC/MS/MS samples for analysis.

5.44. Pharmacokinetic study in SD rats

A33 was dissolved in 0.40 mg/mL 5 % DMSO/95 % (20 % HP-β-CD in water) to make a clear solution. For group I (three male SD rats), **A33** (2 mg/kg) was administered by tail vein injection, and 200 μL blood samples were drawn at 5 min, 15 min, 30 min, 1 h, 2 h, 4 h, 7 h, and 24 h. For group II (three male SD rats), **A33** (10 mg/kg) was administered via oral gavage, and 200 μL blood samples were drawn at 5 min, 15 min, 30 min, 1 h, 2 h, 4 h, 7 h, and 24 h. The blood samples were centrifuged at 3200 g for 10 min, and the plasma was collected for LC/MS/MS analysis.

Declaration of competing interest

The authors declare that they have no known competing financial interests or personal relationships that could have appeared to influence the work reported in this paper.

Acknowledgements

The authors thank Hongwei Liu from the Institute of Microbiology, Chinese Academy of Sciences, for providing the fluconazole-resistant strains of *Candida albicans* (*strain 17#* and *strain CaR*). The authors thank Prof. Yongbing Cao from the School of Pharmacy, the Second Military Medical University, for providing the strain of *Candida albicans* (*SC5314*). This work was supported by the Program for Innovative Research Team of the Ministry of Education and Program for Liaoning Innovative Research Team in University.

Appendix A. Supplementary data

Supplementary data to this article can be found online at https://doi.org/10.1016/j.ejmech.2021.113715.

References

[1] E.M. Carmona, A.H. Limper, Overview of treatment approaches for fungal infections, Clin. Chest Med. 38 (2017) 393–402.
[2] C. Pannuti, R. Gingrich, M.A. Pfaller, C. Kao, R.P. Wenzel, Nosocomial pneumonia in patients having bone marrow transplant. Attributable mortality and risk factors, Cancer 69 (1992) 2653–2662.
[3] P. Fischer, S. Jungwirth, S. Weissgram, K.H. Tragl, Emerging fungal infections among children: a review on its clinical manifestations, diagnosis, and prevention, J. Pharm. BioAllied Sci. 2 (2010) 314–320.
[4] A.H. Groll, J. Lumb, New developments in invasive fungal disease, Future Microbiol. 7 (2012) 179–184.
[5] S. Chunquan, Z. Wannian, J. Haitao, Z. Min, S. Yunlong, X. Hui, Z. Jie, M. Zhenyuan, J. Qingfen, Y. Jianzhong, Structure-based optimization of azole antifungal agents by CoMFA, CoMSIA, and molecular docking, J. Med. Chem. 49 (2006) 2512–2525.
[6] M.A. Pfaller, D.J. Diekema, Epidemiology of invasive candidiasis: a persistent public health problem, Clin. Microbiol. Rev. 20 (2007) 133–163.
[7] D.R. Andes, N. Safdar, J.W. Baddley, G. Playford, A.C. Reboli, J.H. Rex, J.D. Sobel, P.G. Pappas, B.J. Kullberg, G. Mycoses Study, Impact of treatment strategy on outcomes in patients with candidemia and other forms of invasive candidiasis: a patient-level quantitative review of randomized trials, Clin. Infect. Dis. 54 (2012) 1110–1122.
[8] E.W. Bratton, N. El Husseini, C.A. Chastain, M.S. Lee, C. Poole, T. Stürmer, J.J. Juliano, D.J. Weber, J.R. Perfect, Comparison and temporal trends of three groups with cryptococcosis: HIV-infected, solid organ transplant, and HIV-Negative/Non-Transplant, PloS One 7 (2012), e43582.
[9] G.D. Brown, D.W. Denning, N.A.R. Gow, S.M. Levitz, M.G. Netea, T.C. White, Hidden killers: human fungal infections, Sci. Transl. Med. 4 (2012) 165rv13.
[10] S. Arikan, J.H. Rex, Nystatin LF (Aronex/Abbott), Curr. Opin. Invest. Drugs 2 (2001) 488–495.
[11] D. Allen, D. Wilson, R. Drew, J. Perfect, Azole antifungals: 35 years of invasive fungal infection management, Expert Rev. Anti-infect. Ther. 13 (2015) 787–798.
[12] D.W. Denning, Echinocandin antifungal drugs, Lancet 362 (2003) 1142–1151.
[13] V. Moudgal, J. Sobel, Antifungals to treat Candida albicans, Expet Opin. Pharmacother. 11 (2010) 2037–2048.
[14] B.H. Vanden, L. Koymans, H. Moereels, P450 inhibitors of use in medical treatment: focus on mechanisms of action, Pharmacol. Therapeut. 67 (1995) 79–100.
[15] S. Emami, P. Tavangar, M. Keighobadi, An overview of azoles targeting sterol 14α-demethylase for antileishmanial therapy, Eur. J. Med. Chem. 135 (2017) 241–259.
[16] J.C.R. Corrêa, H.R.N. Salgado, Review of fluconazole properties and analytical methods for its determination, Crit. Rev. Anal. Chem. 41 (2011) 124–132.
[17] P. Kale, L.B. Johnson, Second-generation azole antifungal agents, Drugs Today 41 (2005) 91–105.
[18] L. Zhao, L. Tian, N. Sun, Y. Sun, Y. Chen, X. Wang, S. Zhao, X. Su, D. Zhao, M. Cheng, Design, synthesis, and structure-activity relationship studies of l-amino alcohol derivatives as broad-spectrum antifungal agents, Eur. J. Med. Chem. 177 (2019) 374–385.
[19] D. Zhao, S. Zhao, L. Zhao, X. Zhang, P. Wei, C. Liu, C. Hao, B. Sun, X. Su, M. Cheng, Discovery of biphenyl imidazole derivatives as potent antifungal agents: design, synthesis, and structure-activity relationship studies, Bioorg. Med. Chem. 25 (2017) 750–758.

[20] B. Sun, K. Liu, J. Han, L.Y. Zhao, X. Su, B. Lin, D.M. Zhao, M.S. Cheng, Design, synthesis, and biological evaluation of amide imidazole derivatives as novel metabolic enzyme CYP26A1 inhibitors, Bioorg. Med. Chem. 23 (2015) 6763–6773.
[21] M.D.T. Moldes, G. Costantino, M. Marinozzi, R. Pellicciari, Synthesis and preliminary biological evaluation at the glycine(B) site of (+)- and (-)-3-oxetanylglycine, novel non-proteino genic amino acids, Farmaco 56 (2001) 609–613.
[22] M.J. Miller, G.C. Moraski, S.G. Franzblau, Utilization of the Suzuki coupling to enhance the antituberculosis activity of aryloxazoles, Heterocycles 80 (2010) 977–988.
[23] A.J. Phillips, Y. Uto, P. Wipf, M.J. Reno, D.R. Williams, Synthesis of functionalized oxazolines and oxazoles with DAST and deoxo-fluor, Org. Lett. 2 (2000) 1165–1168.
[24] C. Mordant, P. Dunkelmann, V. Ratovelomanana-Vidal, J.P. Genet, A versatile route to syn- and anti-alpha-amino beta-hydroxy esters from beta-keto esters by dynamic kinetic resolution with Ru-SYNPHOS (R) catalyst, Eur. J. Org Chem. (2004) 3017–3026, 2004.
[25] M.C. Myers, J. Wang, J.A. Iera, J.K. Bang, T. Hara, S. Saito, G.P. Zambetti, D.H. Appella, A new family of small molecules to probe the reactivation of mutant p53, J. Am. Chem. Soc. 127 (2005) 6152–6153.
[26] L. Zhao, N. Sun, L. Tian, Y. Sun, Y. Chen, X. Wang, S. Zhao, X. Su, D. Zhao, M. Cheng, Combating fluconazole-resistant fungi with novel β-azole-phenylacetone derivatives, Eur. J. Med. Chem. 183 (2019) 111689.
[27] M.S. Hong, T.W. Kim, B. Jung, S.H. Kang, Enantioselective formation of tert-alkylamines by desymmetrization of 2-substituted serinols, Chem. Eur J. 14 (2008) 3290–3296.
[28] R. Guillon, F. Pagniez, F. Giraud, D. Crepin, C. Picot, M. Le Borgne, F. Morio, M. Duflos, C. Loge, P. Le Pape, Design, synthesis, and in vitro antifungal activity of 1-[(4-substituted-benzyl)methylamino]-2-(2,4-difluorophenyl)-3-(1H-1,2,4-triazol- 1-yl)propan-2-ols, ChemMedChem 6 (2011) 816–825.
[29] C. Muller, U. Binder, F. Bracher, M. Giera, Antifungal drug testing by combining minimal inhibitory concentration testing with target identification by gas chromatography-mass spectrometry, Nat. Protoc. 12 (2017) 947–963.
[30] T.Y. Hargrove, L. Friggeri, Z. Wawrzak, A. Qi, W.J. Hoekstra, R.J. Schotzinger, J.D. York, F.P. Guengerich, G.I. Lepesheva, Structural analyses of Candida albicans sterol 14 alpha-demethylase complexed with azole drugs address the molecular basis of azole-mediated inhibition of fungal sterol biosynthesis, J. Biol. Chem. 292 (2017) 6728–6743.
[31] T. Shimada, H. Yamazaki, M. Mimura, Y. Inui, F.P. Guengerich, Interindividual variations in human liver cytochrome P-450 enzymes involved in the oxidation of drugs, carcinogens and toxic chemicals: studies with liver microsomes of 30 Japanese and 30 Caucasians, J. Pharmacol. Exp. Therapeut. 270 (1994) 414–423.
[32] T. Sakaeda, K. Iwaki, M. Kakumoto, M. Nishikawa, T. Niwa, J.-s. Jin, T. Nakamura, K. Nishiguchi, N. Okamura, K. Okumura, Effect of micafungin on cytochrome P450 3A4 and multidrug resistance protein 1 activities, and its comparison with azole antifungal drugs, J. Pharm. Pharmacol. 57 (2005) 759–764.